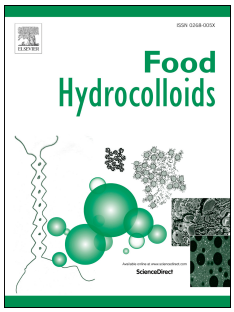

A novel approach for dynamic *in-situ* surface characterisation of milk protein concentrate hydration and reconstitution using an environmental scanning electron microscope

V.L. Cenini, L. Gallagher, G. McKerr, N.A. McCarthy, D.J. McSweeney, M.A.E. Auty, B.M.G. O'Hagan

PII: S0268-005X(19)32749-3

DOI: https://doi.org/10.1016/j.foodhyd.2020.105881

Reference: FOOHYD 105881

To appear in: *Food Hydrocolloids*

Received Date: 29 November 2019

Revised Date: 8 March 2020

Accepted Date: 23 March 2020

Please cite this article as: Cenini, V.L., Gallagher, L., McKerr, G., McCarthy, N.A., McSweeney, D.J., Auty, M.A.E., O'Hagan, B.M.G., A novel approach for dynamic *in-situ* surface characterisation of milk protein concentrate hydration and reconstitution using an environmental scanning electron microscope, *Food Hydrocolloids* (2020), doi: https://doi.org/10.1016/j.foodhyd.2020.105881.

CRediT author statement

V.L. Cenini: Conceptualization, Methodology, Validation, Investigation, Data curation, Writing-original draft preparation, Writing-Reviewing & Editing, Visualization. **L. Gallagher:** Validation, Formal analysis, Writing-Reviewing & Editing. **G. McKerr:** Conceptualization, Funding acquisition, Writing-Reviewing & Editing. **N. A. McCarthy:** Resources, Writing-Reviewing & Editing, Project administration. **D. J. McSweeney:** Formal analysis, Resources, Writing-Reviewing & Editing. **M.A.E. Auty:** Conceptualization, Funding acquisition. Writing-Reviewing & Editing. **B. M. G. O'Hagan:** Conceptualization, Methodology, Funding acquisition, Writing-Reviewing & Editing, Supervision, Project administration.

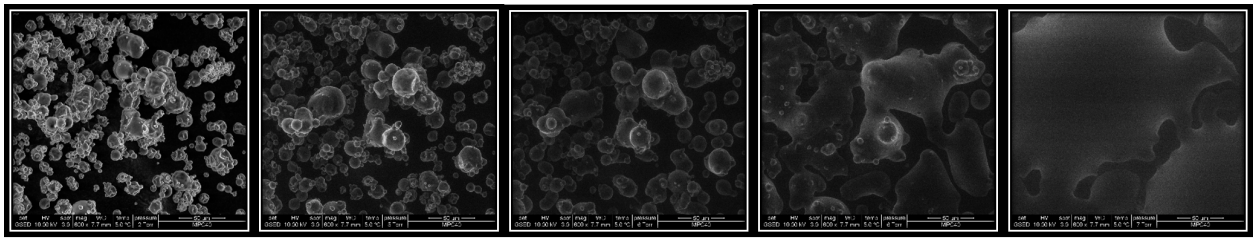

Dry milk powder particles Swelling Fusion Rearrangement Dissolution

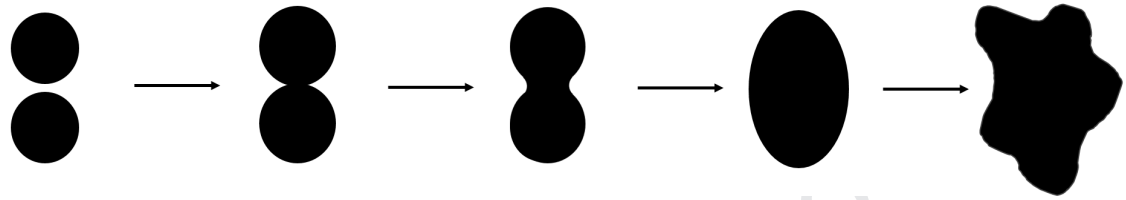

A novel approach for dynamic *in-situ* surface characterisation of milk protein concentrate hydration and reconstitution using an environmental scanning electron microscope

V.L. Cenini[1], L. Gallagher[1], G. McKerr[1], N. A. McCarthy[2], D. J. McSweeney[2], M.A.E. Auty[3], B. M. G. O'Hagan[1]

[1]*Bioimaging Core Facility Unit, Biomedical Sciences Research Institute, Ulster University, Coleraine, BT52 1SA, Northern Ireland, UK*

[2]*Food Chemistry & Technology Department, Teagasc Food Research Centre, Moorepark, Fermoy, Co. Cork, P61 C996, Ireland*

[3] *Mondelez International Ltd., Reading Science Centre, Whiteknights Campus, Pepper Lane, Reading, RG6 6LA, UK*

Corresponding author: Valeria L. Cenini, Bioimaging Core Facility Unit, Biomedical Sciences Research Institute, Ulster University, Cromore Road, Coleraine, BT52 1SA, Northern Ireland, UK, Email v.cenini@ulster.ac.uk, Tel +44 (0)28 701 23074.

Keywords:
Environmental scanning electron microscope; Milk protein concentrate; Surface microstructure; Hydration; Reconstitution; Surface fusion.

Abstract

Composition and relative humidity (RH) can have a profound impact on the physical (flowability, stickiness) and functional (reconstitution) properties of milk powder (MP) and therefore its quality, storage stability and shelf-life. Conventional microscopic techniques are not capable of dynamically imaging the effect of RH on MP at high magnification. The aim of this study was to develop a novel method to characterise *in-situ* and in real time the hydration and reconstitution of five spray-dried milk protein concentrates (MPCs) using an Environmental Scanning Electron Microscope (ESEM). ESEM was employed to observe the surface microstructure of MPC powders with varying protein content (38.63% - 80.94%, w/w), at various RH values ranging from 35% to over 100%. MPC powders were imaged by an ESEM without any prior preparation, and with minimal physical sample alteration, thus providing fundamental insights into MPC hydration and reconstitution. ESEM surface analysis showed particle swelling in all MPCs, and that with increasing protein content, hydration and reconstitution efficiency decreased. For the first time, dynamic particle surface fusion was observed. Such fusion can result in stickiness and caking over time. ESEM methods developed here may provide mechanistic insights into the effects of RH during storage. Surface re-arrangement was also observed in all MPCs, but was impeded in MPC70 and MPC80 thus indicating that this is the rate limiting step for MPC reconstitution. This work validates the use of an ESEM to dynamically characterise MPC powder hydration and reconstitution *in-situ* and in real-time, at both high magnification and spatial resolution.

1. Introduction

In recent years, the consumption and demand for milk powder (MP) as a food ingredient has increased globally and it is expected to continue to grow in the future (Felix da Silva, Ahrné, Ipsen & Hougaard, 2018; Lagrange, Whitsett and Burris, 2015). Due to its nutritional (e.g. high protein, low fat and sugar content), functional (e.g. foaming, viscosity, gelation, emulsification, curd-forming ability and solubility) and sensory properties (e.g. flavour and texture), milk protein concentrate (MPC) has experienced exponential demand as an ingredient in many food products (Felix da Silva et al., 2018).

MPC is a casein-dominant, high-protein dairy powder derivative resulting from membrane separation processes such as ultrafiltration (UF) and diafiltration (DF) of pasteurised skimmed milk followed by spray-drying (Mistry & Hassan, 1991; Mulvihill & Ennis, 2003). Spray dried MPs consist mainly of proteins (caseins and whey), fat, lactose and mineral elements (Mulvihill & Ennis, 2003). Depending upon the degree of UF and DF, the final protein content expressed as a ratio (w/w) vs the dry matter is variable. With increasing protein content, the amount of lactose decreases (Huppertz, Fox & Kelly, 2018; Kelly et al., 2015). Spray-drying fresh milk products has several advantages (stable food reserve with longer shelf-life, better quality, easier storage and transport), but may also strongly affect the physical and chemical properties of the final product (Carić & Keláb, 1987) and, in particular, the relationship the different constituents (lactose and proteins) have with water (Hardy, Scher & Banon, 2002).

As moisture evaporates during the spray-drying process, hydrophobic proteins and fats migrate through the aqueous phase and accumulate at the powder surface, whilst the hydrophilic lactose shifts to the core of the particle (Bhandari, 2013; Gaiani et al., 2006b, 2010; Kelly et al., 2015; Kim, Chen & Pearce, 2002; Nijdam & Langrish, 2006; Shrestha, Howes, Adhikari, Wood & Bhandari, 2007). Such accumulated fat makes the MP surface

hydrophobic and negatively impacts its oxidative stability, flowability, solubility, wettability and dispersibility (Kim et al., 2002; Nijdam & Langrish, 2006; Vignolles Jeantet, Lopez & Schuck, 2007). Surface composition and moisture levels affect the particles' structural and functional properties (Kim, Chen & Pearce, 2005; Nijdam & Langrish, 2006). These in turn have an impact on the handling (e.g. powder blockage in spray dryers, silos and hoppers), storage (e.g. shelf-life issues involving caking) and transport capabilities of MPs (Kelly et al., 2015; Kim et al., 2002; Nijdam & Langrish, 2006).

During spray drying, the rapid cooling and removal of water results in lactose that is normally very hygroscopic and in a solid and unstable glass-like amorphous state. At relatively low temperatures (T°s) and/or relative humidities (RHs), lactose molecules are not able to freely arrange, are more open and porous, and can easily absorb water. However, with increased T° and/or high RH, the molecular mobility of lactose increases and the viscosity decreases, transforming the lactose into a syrup-like, supercooled liquid (glass transition) (Carpin et al., 2016; Haque & Roos, 2004; Thomas, Scher, Desobry-Banon & Desobry, 2004). During manufacture, packaging, storage and transport, the control of T° and RH is very limited (Hardy et al., 2002; Maidannyk et al., 2020). At high moisture levels, lactose is released from the particles' surface, and, due to capillary forces and surface tension, merges with adjacent particles at contact points forming viscous liquid bridges. This can result in the onset of sticking and caking, decreased flowability and lactose crystallisation (Aguilera, del Valle, & Karel, 1995; Bhandari, 2013; Carpin et al., 2016; Crowley, Gazi, Kelly, Huppertz & O'Mahony, 2014; Haque & Roos, 2004; Hardy et al., 2002; Hogan & O'Callaghan, 2010; Lloyd, Chen & Hargreaves, 1996; Palzer, 2005; Peleg, 1977). These bridges can later solidify by drying, cooling, melting and fusion, crystallisation to form solid bridges (Bhandari, 2013; Hardy et al., 2002; Peleg, 1977). The quality of the product is therefore diminished, leading to significant economic loss (Aguilera et al., 1995; Carpin et al., 2016). Lactose crystallisation is

delayed in the presence of protein due to its preferential water sorption (Hogan & O'Callaghan, 2010; Kelly et al., 2015; Maidannyk et al., 2020). At constant T°, lactose crystallisation is dependent upon RH, time, and particle water content. It is indicated by a loss of sorbed water as a function of time (Haque & Roos, 2004; Hogan & O'Callaghan, 2010; Jouppila & Roos, 1994; Jouppila, Kansikas & Roos, 1997; Thomas et al., 2004). Lactose crystallisation may also damage the milk fat globule membrane and the proteins that encapsulate the fat droplets. Once released, the fat droplets migrate to the surface, especially in a humid environment, adding to the hydrophobicity of the surface (Aguilar & Ziegler, 1994; Saito, 1985; Thomas et al., 2004).

The withdrawal of moisture from milk has been shown to have no effect on whey proteins, but alters casein protein molecular conformation to a more hydrophobic form. This conformational modification, and water-protein interactions at the particle surface, eventually lead to decreased solubility (Baldwin, 2010; Haque et al., 2010; Haque, Bhandari, Gidley, Deeth & Whittaker, 2011; Ikeda, 2015). During milk spray-drying, lactose takes the place of the lost water molecules, thus maintaining the native structure of the proteins in MPs (Baldwin, 2010; Thomas et al., 2004). Therefore, hydrogen bonds between carbohydrates and dry proteins are an important factor in protein stability during dehydration and also during their subsequent hydration and reconstitution (Baldwin & Truong, 2007). Water-holding capacity, often termed water hydration capacity or swelling capacity, is the ability of the casein micelles (CMs) to bind, entrap or retain large amounts of water under defined conditions. Such capacity and reconstitutability of milk proteins are important functional properties for food formulations (Davenel, Schuck & Marchal, 1997; Kneifel, Paquin, Abert & Richard, 1991; Kneifel & Seiler, 1993; Zayas, 1997).

Poor reconstitution and incomplete dissolution properties of MPC powders are major limiting factors in maximising their utility as a food ingredient and may have a deleterious impact on

the quality of the product (Crowley, Kelly, Schuck, Jeantet, O'Mahony, 2016; Forny, Marabi & Palzer, 2011; Ikeda, 2015; Mimouni, Deeth, Whittaker, Gidley & Bhandari, 2010b; Schuck et al., 2007).

Increasing protein concentration in MPCs is well-documented as having a detrimental impact on its solubility and on one or more of the reconstitution stages: wetting, swelling, sinking, dispersion and dissolution (Gazi & Huppertz, 2015; McKenna, 2000; Mimouni, Deeth, Whittaker, Gidle, & Bhandari, 2009; Sikand, Tong, Roy, Rodriguez-Saona & Murray, 2011). Although the exact mechanism of MPC powder insolubility is not fully established, several theories have been proposed, particularly in relation to high-protein content MPCs. These suggest that an increase in predominantly casein protein-protein hydrophobic interactions is formed on the surface of the particles inhibiting their dissolution (Anema, Pinder, Hunter & Hemar, 2006; Fang, Selomulya, Ainsworth, Palmer & Chen, 2011; Fyfe et al.,2011a; Havea, 2006; Haque et al, 2011; McKenna 2000;Mimouni et al., 2009). The interaction between CMs could explain why high-protein and casein-dominant powders such as MPC have difficulty dispersing (Bouvier, Collado, Gardiner, Scott & Schuck, 2013; Gaiani, Banon, Scher, Schuck & Hardy 2005; Gaiani, Schuck, Desobry & Banon, 2007; Schuck et al., 2007). However, the exact mechanism of hydration and reconstitution remain poorly understood (Felix da Silva et al., 2018).

The food industry have long recognised the potential of microstructural analysis to examine the functional properties of MPs, in particular its hydration and reconstitution characteristics. These strongly correlate with structural features such as surface morphology, structure, heterogeneity, and chemical composition (Burgain et al., 2017). It is well established that lactose and protein content in MPs have a significant impact on the surface microstructure as well as physicochemical and structural properties of MP particles (Mistry, Hassan & Robinson, 1992). The combined surface properties of MPs play a pivotal role in several of the

reconstitution stages such as wetting, dispersion and dissolution (Murrieta-Pazos et al., 2012), therefore, it is imperative to identify the rate-limiting steps affecting MP characteristics and functional properties (Forny et al., 2011).

Light and electron microscopy are amongst the most frequently used microscopical techniques for investigating food microstructure, not only due to the highly intuitive imagery, but also due to the generation of numerical data for statistical analysis (Auty, 2018; Crowley et al., 2016; Kelab, 1981; Kelab, Allan-Wojtas & Miller 1995; Murrieta-Pazos et al., 2012). Whilst optical microscopy affords the possibility for dynamic studies with minimal sample preparation, resolution and hence magnification are limited. Since the 1950s, conventional high vacuum Scanning Electron Microscopy (SEM) has become an increasingly useful tool for visualising food microstructure, offering high spatial resolution and magnification, orders of magnitude beyond what is achievable with optical microscopy. Due to the inherent nature of high vacuum SEM, samples cannot be imaged in their natural or hydrated state. SEM often requires varying sample preparation depending on the sample of interest such as freeze drying, critical point drying, deposition of a conductive coating and, in some cases, chemical fixation. Such preparation could be time consuming and can obscure or profoundly alter the sample, having implications for surface morphology, microstructure and in rare cases compromise the integrity of the sample. This may result in reduced experimental reproducibility (Fang, Selomulya & Chen 2010) and the introduction of artefacts (Kelab, 1979; 1984), including shrinkage and collapse (Timp & Matsudaira, 2008). In addition, samples processed in this way are effectively ‘fixed’ in space and time, and so are unsuitable for dynamic experiments (James, 2009).

The Environmental Scanning Electron Microscope (ESEM) evolved from conventional high vacuum SEM (Danilatos, 1985; 1991). ESEMs strength lies in its ability to image samples directly with no sample preparation needed, allowing for the circumvention of many of the

limitations and damaging effects imposed by conventional SEM. ESEM is a versatile and well established tool, used extensively to image a diverse range of hydrated materials, from plants, animals, micro-organisms, living cells (Tai & Tang, 2001), to chocolate (James & Smith, 2009) and skin care emollients (Antonijevic, Novac & O'Hagan, 2018). ESEM utilises gaseous secondary electron detectors and inert gases to amplify the secondary electron signal and to create a much more water compatible imaging environment (Danilatos, 1985; Strokes, 2013). By combining a multistage differential pumping system and a series of pressure-limiting apertures within the column, the electron source and gun are kept at high vacuum (low pressure; 10^{-6}-10^{-7} Torr), whilst maintaining relatively low vacuum conditions (high pressure; 1 to 20 Torr) within the specimen chamber (Danilatos, 1985; Donald, 2003). Vapour pressure is controlled by deploying water vapour as the inert gas whilst T° is independently manipulated with the use of a Peltier cooling stage. This permits a full range of RH values at the level of the specimen to be achieved and maintained (Danilatos, 1985; Garcia-Salinas & Donald, 2010). ESEM combines and complements the best features of ultra-high vacuum SEM and light microscopy to provide a non-invasive, non-destructive and often label-free technique that can be used to dynamically analyse and characterise food surface microstructure such as MP (James, 2009). In particular, it can be used to monitor sample's hydration *in-situ* and to image fully hydrated samples (Garcia-Salinas & Donald, 2010). Dairy powders have been imaged in ESEM to obtain morphological parameters, including particle size and shape (Perea-Flores et al., 2010) and, in conjunction with EDX, elemental analysis of MP surface (Murrieta-Pazos, Galet, Rolland, Scher & Gaiani, 2013). To the best of our knowledge, the work described here is the first to employ ESEM to observe and characterise in real-time, the *in-situ* hydration and reconstitution of MPC powder. The aim of this research was to develop a novel method to elucidate the changes on the surface and

microstructure of MPCs, induced by real time changes in RH to better understand MPC powder behaviour during storage and reconstitution.

2. Materials and Methods

2.1 MPC powder manufacture

MPC powders were produced in the Bio-functional Food Engineering Facility at Teagasc Food Research Centre (Moorepark, Fermoy, Co.Cork). Liquid MPC (21.1% and 17.6%, w/w, total solids and protein, respectively) and concentrated milk permeate (24.2%, w/w, TS) were obatined from a local dairy supplier directly after ultrafiltration and reverse osmosis, respectively. Milk permeate was then re-added to the ultrafiltration retentate so as to dilute the protein content to ~40, 50, 60 or 70%, w/w, protein. The subsequent five (i.e., MPC40, 50, 60, 70 and 80) MPC batches were stored overnight at 4 °C under gentle agitation. The total solids content of the MPC40, 50, 60, 70 and 80 concentrate was 22.6, 22.4, 22.5, 21.0, and 21.6%, respectively. MPC batches were pre-heated to 45 °C and spray dried using a single-stage spray dryer (Anhydro F1 Lab Dryer; Copenhagen, Denmark) equipped with a two-fluid nozzle atomisation system (Type 1/8 JAC 316ss) under counter-flow drying conditions. The atomization pressure was set at ~2 – 3 bar. Air inlet and outlet T°s were maintained at 185 and 80 °C, respectively.

2.2 MPC characterisation and composition

The protein content of MPC powders was obtained by the Dumas method using a LECO FP628 nitrogen analyser (LECO Corporation, St Joseph, Michigan, USA). This was determined by multiplying the nitrogen concentration by a nitrogen-to-milk protein conversion factor of 6.38. The fat content of MPC powders was analysed using the Rose Gottlieb method. The free moisture and ash content of the MPC powders was determined

using a TGA701 thermogravimetric analyser (LECO Corporation, St Joseph, Michigan, USA). The lactose value was calculated by difference. All analysis were carried out in triplicate except for fat determination, which was performed in duplicate.

The samples used in this study were characterised by increasing protein levels (from 38.6% to 80.9% w/w) and consequently a substantially decreased lactose content (from 51.1 % to 6.31 % w/w; Table 1). The fat content more than doubled from 0.6% w/w for MPC40 to 1.5% w/w for MPC80. All samples were stored in a refrigerator at 5°C in sealed containers and opened immediately before the experiment.

2.3 ESEM: establishment of operational conditions

All microscopy related work was performed at Ulster's Bio-Imaging Core Facility Unit, using a FEI Quanta^{TM} 200 ESEM (FEI Company, Eindhoven, Netherlands) equipped with a 500µm aperture gaseous secondary electron detector (GSED) and a Peltier cooling stage. Water vapour was used as the imaging gas. Images were acquired via the integrated imaging software (xT microscope control) and a charge coupled device camera. The image sequences were converted to video format using Adobe Photoshop CS6.

Prior to imaging, initial chamber purge parameters, operational chamber pressure and sample T° values were established and optimised to allow for continuous imaging with minimal sample damage. A T° of 5^{o}C was selected and used throughout this study. To monitor MPC powder hydration, all samples were imaged at a starting RH of 35% (2.3 Torr at 5°C). To achieve MPC sample equilibrium, an initial chamber purge sequence (2 purge cycles ranging from 1.8 Torr to 2.3 Torr) was performed to allow water vapour to replace the air in the chamber at near atmospheric pressure. RH was controlled by adjusting the vapour pressure within the chamber. Accelerating voltage of 10kV, spot size 3, working distance of 8±1mm and 0.3 ms scanning speed delivered optimal imaging conditions. A magnification of 3000x

or 6000x was used for obtaining detailed particle surface morphology. A magnification of 1200x was selected for all the dynamic experiments, as it encompassed a useful number of particles at a resolution which permitted the observation of crucial features, with minimal beam damage under continuous imaging conditions. The experiments described in this report were repeated in triplicate and the images presented are from one single representative experiment.

2.3.1 Dynamic in-situ MPC powder hydration and reconstitution

Using a spatula, MPC powders were sprinkled onto double-sided adhesive carbon tape attached to 3/8inch (~10 mm) diameter copper ESEM stubs (3205c Agar Scientific, Stansted, UK). The stub was then inserted into a pre-cooled (5^{o} C) Peltier cooling stage within the ESEM chamber. Purge cycles were initiated in order to establish initial chamber conditions (35% RH). RH was then increased in 5% increments by increasing vapour pressure in steps of 0.3 ± 0.1 Torr at 5 minutes intervals (Table 2). Vapour pressure was increased until RH exceeded 100% (>100% RH, 6.8 Torr). At this point, water started to form on the sample and stub surface, eventually covering the entire stub with water (Fig. 1; Fig. S1). Samples were maintained under these conditions for 30 minutes. Brightness and contrast settings were adjusted accordingly to ensure image quality.

2.3.2 Dynamic in-situ MPC powder dehydration

After 30 minutes at >100% RH, vapour pressure within the chamber was returned to the initial 35% RH value, returning the sample to “dry” conditions and allowing the resulting residue to be imaged.

3. Results

3.1. Initial MPC powder surface microstructure characterised by ESEM

Each of the MPC powder samples displayed spherical shape and showed a heterogeneity of particle morphology with small particles often found within the folds of the larger ones (Figs. 2 to 7). Some of the MPC40 particles' surface were smooth (Figs. 2a; 3), but the majority of particles presented a wrinkled appearance. They often showed deep and large surface folds/dents and displayed a deflated appearance. The particle surface of MPC50 (Figs. 2b; 4) and MPC60 (Figs. 2c; 5) was smoother than MPC40 with folds. MPC70 (Figs. 2d; 6) and MPC80 (Figs. 2e; 7) particles displayed a much more spherical appearance, folds were still present, and the surface only very occasionally presented with wrinkles.

3.2 MPC powder hydration

All the results are summarised in Table 3 and the full hydration process of MPC40 to 80 can be viewed in videos 1 to 5 (respectively) in the electronic version.

3.2.1 MPC40

In MPC40, complete hydration at 5°C was clearly observed in all MP particles (Fig. 3). Starting at 35% RH, with increasing RH, a few particles displayed only slow movement (Fig. 3a) with no obvious change in size or surface morphology. At 50% RH, milk particles started to slowly swell (Fig. 3b). At higher RH (75%-80%), significant conformational changes occurred to the particles (Fig. 3c). At this RH, MPC40 particles showed a sudden and rapid increase in size, folds disappeared, and the particles' surface appeared fuller and rounder, with a smoother overall superficial appearance. With increasing RH, particles continued to swell rapidly and, just before reaching 100% RH (90-95% RH), adjacent particles started to gradually "fuse" together (Fig. 3d). It was noted that some of the particles deflated just before

the fusion phase. At 100% RH, particle fusion increased, with surface re-arrangement being evident (Fig. 3e). During the surface fusion and re-arrangement, holes present on the particle surface (Fig. 3b, 3c, 3d, white arrows) closed over prior to dissolution (Fig. 3e). As the sample approached 100% RH, particle shape and definition were completely lost, continuing to enlarge with time (Fig. 3f). From the micrographs, it can be noted that the majority of the small particles were the last to break up (Fig. 3e), losing their structural integrity at saturated water vapour pressure (>100% RH; Fig. 3f). MPC40 exhibited fast and efficient hydration, and when the RH exceeded 100%, the particles started to quickly dissolve.

3.2.2 MPC50 and MPC60

From 35% RH, MPC50 and MPC60 a few particles showed only slow movement and started to swell at 50% RH (Figs. 4a, 4b; 5a, 5b respectively). Significant and rapid changes in swelling were observed at 80-85% RH for MPC50 (Fig. 4c) and 85-90% RH for MPC60 (Fig. 5d). In MPC50 particles, the fusion and re-arrangement was evident below 100% RH (90-95%; Fig. 4d), whilst for some of the MPC60 particles it was observed at 100% RH (Fig. 5e). In the case for both MPCs, slight particle deflation was noted prior to surface fusion, with surface fusion and re-arrangement occurring rapidly. The particles continued to rearrange until they completely lost their shape at >100% RH (Figs. 4f; 5f).

3.2.3 MPC70 and MPC80

In MPC70 and MPC80, starting from 35% RH (Figs. 6a; 7a respectively), particle movement was much less noticeable than in the other MPCs. The particles started to slowly swell at 50% RH (Fig. 6b; 7b) and showed less pronounced particle size increase during the swelling stage at 85-90% RH (Figs. 6d; 7d). No deflation was observed in these powders. For MPC70 particles, surface fusion and re-arrangement started at 100% RH (Fig. 6e), and for MPC80 it

occurred only at RH values in excess of 100% (Fig. 7f). This stage progressed slowly and with difficulty, and the surface folds disappeared only at >100% RH. At saturated water vapour pressure, MPC70 particles started to lose shape, and this process took much longer in the case of MPC80 particles, which appeared to float on top of the water as it formed (Fig. S2).

3.3 MPC powder dehydration

Micrographs of MPC40 at 35% RH show a fairly uniform and smooth residue with all the particles dissolved (Fig. 8f). In the case of MPC50, and in particular MPC60 (Figs. 8g, 8h respectively), the residue had a more granular appearance indicating a larger amount of undissolved particles. MPC70 residue showed a greater amount of undissolved particles with a flattened and elongated appearance, nonetheless their shape was still recognisable (Fig. 8i). MPC80 residue exhibited considerably more undissolved particles with their original spherical morphology still being recognisable (Figs. 8j, 9b).

4. Discussion

The five powders were prepared from the same milk composition and under the same processing conditions, therefore eliminating variations in casein structure and the resulting variability in hydration and reconstitution properties usually found among different MPC products (Felix da Silva et al., 2018). Consequently, these samples afford the possibility of providing insights into MPC powder morphology, hydration and reconstitution as a function of the protein, lactose and fat content (Gazi & Huppertz, 2015).

The low vacuum conditions and the absence of a conductive coating within ESEM, permits imaging of MPC powder samples directly in their dry state. A T° of 5° C was used to mimic MP hydration and reconstitution at a T° consistent with standard refrigeration (Baldwin,

2010). It was also used to minimise moisture loss (Stokes, 2013) and avoid destructive ice crystal formation (Buckman, 2000), whilst allowing the use of modest gas pressures (6.8 Torr maximum; Fig.1; Table 2). This ensured good signal to noise ratio and high spatial resolution (Donald, 2003; Stokes, 2012; Tai & Tang, 2001) whilst minimising the damage to beam sensitive colloidal material such MPC and to allow water droplets to form on the sample surface (Kitching & Donald, 1998). Prolonged ESEM imaging at higher T° necessitates increasing vapour pressures in order to achieve target RH values. In addition to placing considerable stress on the instrument, it results in a rapid degradation of image quality. These conditions necessitate the use of higher accelerating voltages, which with repeated and prolonged imaging, may result in damage to, or alteration of the sample. 5^{o} C was found to be a useful compromise T°.

MPC powder morphology observed by environmental scanning electron microscopy correlates with previous observations made with high vacuum SEM (Kelab, 1979; Kelly et al., 2015; McSweeney, Maidannyk, Montgomery, O'Mahony & McCarthy; 2020; Mimouni, Deeth, Whittaker, Gidley & Bhandari, 2010a; Thomas et al., 2004; Vos et al., 2016). All five MPC powder samples used in this study displayed a typical spherical shape and heterogeneity of particle size (Figs. 2 to 7). MPC40 particles displayed a more deflated appearance compared to MPCs with higher protein content such as MPC80, which instead appeared much rounder. This may be due to a low volume of interstitial and occluded air found in low protein content MPC powders, which increases with increasing protein content (Crowley et al., 2014; Kelly et al., 2015).

ESEM analysis showed that all five powders exhibited large dents/folds (Fig.2, yellow arrows), indicative of high surface protein coverage due to the spray drying process (Buma and Henstra, 1971; Fäldt & Bergenståhl, 1994; Gaiani et al, 2006b; Mistry et al., 1992). The powders' surface also showed some morphological differences. MPC40 (Figs. 2a; 3) particles

often displayed deep wrinkles on the surface (Fig.2, light blue arrow) indicative of a high lactose content and/or minimal superficial fat content (Kelly et al., 2015; Mistry et al., 1992). The particle surface of MPC50 (Figs. 2b; 4), MPC60 (Figs. 2c; 5), MPC70 (Figs. 2d; 6) and MPC80 (Figs. 2e, green arrow; 7) became increasingly smooth, indicative of a decrease in lactose content and increasing protein concentration (Fäldt & Bergenståhl, 1994; Fyfe, Kravchuk, Nguyen, Deeth, & Bhandari, 2011b; Kelly et al., 2015; Mistry et al., 1992).

MP is a complex system, where proteins, lactose and salts compete for moisture sorption (Berlin, Anderson & Pallansch, 1968; Thomas et al., 2004). The physical and reconstitution properties of MPs depend on moisture and water binding to these components (Hardy et al., 2002). For the first time using an ESEM, the morphological changes that single particles undergo during water vapour sorption (hydration) and in the presence of physical water (>100%RH, reconstitution) have been recorded (Figs. 3 to 7). Two of the five stages of MPC powder reconstitution have been clearly observed and identified. The swelling stage was indicated by changes in particle size and morphology, and the dissolution stage by loss of particle shape and definition.

From 35-45% RH, all MPC particles exhibited no obvious morphological change. At RH values higher than 30%, water molecules are adsorbed on the MP's surface and associate loosely with protein and lactose (Carpin et al., 2016; Schuck, 2011). Water is preferentially sorbed by caseins at low RHs, and by lactose and salts at higher RHs (Berlin et al., 1968; Haque & Roos, 2004). Depending on protein composition, temperature, ionic strength, salt, and pH, water is bounded and entrapped in the capillaries between protein particles (Schuck, 2011). The minor movement observed in some MPC particles within ESEM before the swelling stage could be attributed to the slow water entry as found in Vos et al. (2016). In MPC70 and MPC80, the particle movement and initial swelling due to water entry was much less noticeable than in the other MPCs. This is confirmed by other work looking at the same

(Maidannyk et al., 2020) or similar (McSweeney et al., 2020) MPC powders, where the authors reported that MPC40-60 have a higher rate of water diffusion and wettability than higher protein powders. Moisture sorption is facilitated by hydrophilic lactose that acts as a channel for moisture transfer within the CM and as a spatial separator, disrupting the direct interaction of the hydrophobic ends of adjacent casein molecules (Baldwin, 2010; Gazi & Huppertz, 2015). Therefore, with increasing protein and decreasing lactose, there are fewer hydrogen bonds between lactose and proteins, which can hinder the water-holding capacity (or swelling capacity) of the CMs, as there are more hydrophobic interactions between the micelles eventually leading to impaired solubility. Furthermore, in spray-dried high-proteins powders, protein and fat coverage is overrepresented at the powder surface compared with the bulk composition, adding to the hydrophobicity of the surface (Fyfe et al., 2011b; Kelly et al., 2015; Gaiani et al., 2006b, 2010; Kim et al., 2002; Nijdam & Langrish, 2006). With increasing protein content, the fat content increases at the surface levels (Kelly et al., 2015), and because it is not a water-absorbing component, moisture absorption decreases (Thomas et al., 2004). Therefore, higher levels of surface fat in MPC70 and MPC80, reduces the transfer of water and therefore negatively impacts their solubility (Crowley et al., 2015; Gaiani et al., 2006b, 2010; Schuck et al., 2007; Vignolles et al, 2007).

Using rheological, turbidimetry, static light scattering methods and light microscopy, Gaiani et al. (2006a; 2007) identified in casein-dominant MPs a distinct swelling stage during the hydration process. Yet, such methods have been unable to observe in real time and at high magnification and resolution the morphological changes which occur during this stage. The dynamic *in-situ* hydration experiments characterised the swelling stage of all the MPCs considered in this work, at various RH values. This research shows that the swelling stage is a continuous phase that commences in all powders at 50% RH; at this RH the swelling is minimal and progresses much faster at higher RH values. During the swelling stage, with

increasing RH, each of the MPCs powders manifested a sudden, significant and rapid expansion, occasionally followed by a deflation, which precedes the next step (fusion). This transitional phase has been observed for the first time using the methods presented herein, and it is slowed down with increasing protein content. High protein content powders (MPC70-MPC80), also exhibited a less pronounced change in particle morphology than in lower protein content MPC powders. In MPC40 the transitional phase was observed at 75-80% RH (Fig. 3c), in MPC50 at 80-85% RH (Fig. 4c) and in MPC60, MPC70 and MPC80 at 85-90% RH (Figs. 5d; 6d; 7d respectively). The fact that the swelling stage starts at similar RH and happens in all of the MPC powders, supports the theory that the swelling stage is not the rate-limiting step for MPC powder hydration (Crowley et al., 2016).

With RH increase, the T^o at which the lactose changes state from glass to crystalline (glass transition temperature, $T_{g)}$ decreases (Fitzpatrick et al., 2007). The adsorbed water of amorphous lactose is released during the process of crystallisation (Carpin et al., 2016) and is taken up by the other components, such as proteins (Lai & Schmidt, 1990; Warburton & Pixton, 1978), resulting in a further swelling. With increasing protein, T_g increases and therefore the onset of lactose crystallisation is delayed or prevented, possibly because the proteins hinder the lactose molecules' mobility or lowers water availability for lactose crystallisation (Hogan & O'Callaghan, 2010; Kelly et al., 2015; Maidannyk et al., 2020; Thomas et al., 2004). MPC powder swelling is therefore delayed or is diminished. This may explain why the transitional phase starts at slightly lower RHs in low protein content powders. The fact that the samples showed deflation after the transitional phase, is due to the collapse of the amorphous structure and, therefore, the protein/lactose/fat matrix, that leads to the supercooled liquid state (Carpin et al., 2016; Maidannyk et al., 2020; Murrieta-Pazos et al., 2011). Subsequently, lactose crystallisation may take place (Carpin et al., 2016).

Lactose crystals were not observed at any time on the powder surface. With this technique, we are limited to observations at the level of the particle surface. Ongoing processes within the particle interior may take some time to manifest observable changes at the particle surface (Saito, 1985). With time, lactose crystallisation also releases the free fat encapsulated in fat globule membranes and proteins, creating a barrier at the surface, hindering crystal formation (Aguilar & Ziegler, 1994; Murrieta-Pazos et al., 2011; Saito, 1985; Thomas et al., 2004).

In recent work on the same MPC powder samples as were used in this study, moisture sorption isotherms of the MPC powders showed that only MPC40 and MPC50 displayed clear lactose crystallisation above RH of 54.5% and 85% (respectively) at the T° of 21 ± 2°C (Maidannyk et al., 2020). The experiments performed in this study have been carried out at a constant 5°C, so lactose crystallisation would be expected to occur at higher RH values (Lloyd et al., 1996; Thomas et al., 2004).

For the first-time, during *in-situ* hydration of MPC particles, we have dynamically imaged fusion events, followed by re-arrangement of the particles' surface. Whilst we have observed this process in all of the MPC powders used in this study, the surface fusion and re-arrangement occurred at different RH values, starting at higher RH with increasing protein content (Table 3). In MPC40 and MPC50 the fusion stage was observed at 90-95% (Figs. 3d; 4d respectively), in MPC60 at 95-100% (Fig. 5e), in MPC70 at 100% (Fig. 6e) and MPC80 at over 100% RH (Fig. 7f). During water absorption, the change of state of amorphous lactose at constant T° is irreversible and is dependent upon RH, water content and time (Jouppila et al., 1997; Roos & Karel, 1992). Crystallisation occurs with a decrease in viscosity and higher molecular mobility (Jouppila et al., 1997), and it is preceded by the formation of viscous liquid bridges between powder particles (Fitzpatrick et al., 2007; Peleg, 1977). The particle fusion observed in this study is therefore most likely due to the changing state of lactose from an amorphous solid to a viscous liquid that, with increasing RH at constant T°, is released

from the particles' surface. Once released, lactose merges with adjacent particles forming viscous liquid bridges. These particle-particle interactions can cause stickiness and reduced flowability with time and in turn lead to powder handling and caking problems (Hardy et al., 2002). There is also evidence that milk fat can melt forming viscous liquid bridges (Peleg, 1977), however, this is unlikely to have occurred in our study (Foster, Bronlund & Paterson, 2005) because of the low temperature (5^{o} C) used in our experiments. MPC powder caking was confirmed (in the same powders as used in this study) by Maidannyk et al. (2020), by an increase in particle size as found in MPC40 and MPC50 kept at RH >76 % at 21 ± 2°C. The same was observed in skim milk powder (SMP) but occurred at RH >54% (Murrieta-Pazos et al., 2011). Within ESEM, MPC70 particles started to fuse together at 100% (Fig. 6e) and MPC80 particles at over 100% RH (Fig. 7f), but particle merging is very limited due to decreased lactose content and increased protein and fat content. This is confirmed by Maidannyk et al. (2020), who showed that MPC60-80 powders displayed very little (MPC60) or no (MPC70-80) lactose crystallisation at any RH (from 11% to 85%). The viscous liquid bridges can later solidify forming solid bridges that have high strength and lead to powder agglomeration (Bhandari, 2013; Palzer, 2005; Peleg, 1977). Light, electron and scanning probe microscopy have been used as tools to characterise spray-dried milk stickiness and caking over time (Aguilera et al., 1995; Carpin et al., 2016; Lai & Schmidt, 1990; Prime et al., 2011). Bridging between dry MP particles stored at 79% RH (Aguilera, 1999), SMP particles stored at RH ≥74% (Lai & Schmidt, 1990), whole milk powder with altered lactose content (Aguilar & Ziegler, 1994) and spray-dried amorphous lactose (Lloyd et al., 1996) have been observed by SEM. This is the first study to observe dynamically, and at high magnification and resolution, the effect of RH on MPC powder and the dynamics that can lead to stickiness and caking.

The release of lactose leaves a gap where the superficial proteins, especially CM, are free to re-arrange, before they are released by erosion from the particle surface during the dissolution stage (Mimouni et al., 2009). Casein re-arrangement has been observed in micellar casein powders stored at high temperature (Burgain, Scher, Petit, Francius, & Gaiani, 2016). In MPC40, surface re-arrangement happened immediately after the RH is increased to 100% RH (6.5 torr; Fig.3e) and the process was rapid and continuous. The holes present on the surface of MPC40 particles (Fig. 3b, 3c, 3d, white arrows) completely closed over prior to dissolution. In ESEM, at RH in excess of 100% (6.8 torr; Fig.3f), water droplets form on the sample stub around the particles. With time these droplets grow in size and number, often coalescing into larger droplets, and ultimately forming a single bead (Fig. S1). At this point, it is possible to observe dynamically and *in-situ* the effects of water on MP dissolution, and the particle-water interactions that influence MP reconstitution (Hardy et al., 2002).

The methods described here also afford the opportunity to examine the resulting residue, left after MPs have been returned to the initial 35% RH value, following hydration and reconstitution experiments (Fig. 8, 9). Whilst this is not a reversal of the hydration and reconstitution process, it provides a sense of the extent to which the particles have dissolved. MPC40 particles immediately and completely dissolved at RH in excess of 100%. This is supported by the uniform appearance of the residue left after the sample has been returned to a “dry” state post dissolution. In MPC50 and MPC60 surface re-arrangement still occurred, but it was slowed down, possibly due to decreased lactose content and increased interaction between and within the CMs, and the retarding effect this has on the dissolution stage (Gazi & Huppertz, 2015; McSweeney et al., 2020). Crowley et al. (2015) measured the sediment after centrifugation of MPCs of varying protein content after 90 minutes of hydration at 25°C. They found that MPC35 and MPC 50 powders did not form any sediment, whilst sediment started to form in MPC60 and increased with increasing protein content. ESEM analysis of

the residue of MPC50 post dissolution (Fig. 8g) displayed some undissolved particles as compared to MPC40, a phenomenon perhaps unnoticed in larger scale experiments. MPC60 residue (Fig.8h) displayed an increased number of incompletely dissolved particles. In MPC70 and MPC80, surface re-arrangement was further slowed down, thus leading to incomplete powder dissolution. As with particle fusion, the rate of surface re-arrangement was retarded with increasing protein content, and it was limited in high protein and low lactose content powders such as MPC70 and MPC80. This is possibly due the increased protein and fat migrated to the particle surface during spray-drying that increased the particle surface hydrophobicity (Gaiani et al., 2006b; 2010; Kelly et al., 2015). In fact, in less soluble MPC70 and MPC80, we observed a further increase in undissolved particles in the residue left post dissolution. MPC80 particles in particular, maintained their original morphology. In these powders, single particles started to change shape and fuse together, but this process was incomplete forming a block of fused (MPC70; Fig. 8i) or semi-fused (MPC80; Fig. 8j) particles of larger size, that further retarded hydration. Crowley et al. (2015) found that MPC70 and MPC80 had a large quantity of poorly-dispersible particles in their sediment mainly composed of casein proteins (McKenna, 2000; Anema et al., 2006; Havea, 2006). In agreement with Mimouni et al. (2009), results here suggest that the rate-limiting step for MPC powders is the release of CM from the powders' surface and more specifically the superficial re-arrangement. Our data is supported by other research using transmission electron microscopy (TEM; McKenna, 2000) and field emission scanning electron microscopy (Mimouni et al., 2010a) which show the aggregation or fusion of CM of rehydrated MP particles and the formation of "intermicellar bridges". Within an ESEM we were able to dynamically observe in real time MPC powder hydration and reconstitution showing superficial particle re-arrangement, reflecting what has been observed by TEM inside the MP.

For the first time, using environmental scanning electron microscopy, it was possible to characterise distinct hydration and reconstitution profiles for MPC powders. The findings of this research are consistent with previous studies which have investigated MPC hydration and reconstitution at larger scale (Crowley et al., 2015; Fitzpatrick et al., 2007; Hogan & O'Callaghan, 2010; Kelly et al., 2015; Maidannyk et al., 2020). They show that low- and medium- protein content MPC powders have good hydration and reconstitution properties, compared to high protein content powders.

5. Summary and conclusion

This work has validated the use of an ESEM as a powerful and useful tool to characterise MPC powder hydration and reconstitution in real-time at high magnification and spatial resolution. ESEM analysis has verified that with increasing protein content MPC hydration is greatly impeded and that high protein content powders, in particular MPC80, retain their initial morphology and displayed poor solubility even after reconstitution. This research has shown that there is a transitional phase during the swelling stage, indicated by a sudden and rapid particle size increase. Particle surface fusion has been observed in all MPCs, but it was more evident in low protein content powders. These are more susceptible to lactose crystallisation at high RH and therefore more prone to sticking and caking during storage. The protocols described herein may be of benefit in gauging the degree to which any given sample of MPC may be prone to stickiness and caking. This work has demonstrated that MPC particle surface re-arrangement may be the rate-limiting factor for hydration. These events may be key drivers in particle dissolution and warrant further investigation. This novel research supports and adds to the established body of knowledge within the dairy industry. The ESEM methodologies presented here have provided new and fundamental insights into the mechanisms of MPC powder hydration and reconstitution.

6. Acknowledgements

This original research was supported by the Food Institutional Research Measure (FIRM) project "Developing the next generation of high protein spray dried powders with enhanced hydration properties" (DAIRY DRY 15-F-679), funded by both the Irish Department of Agriculture, Food and the Marine and the Department of Agriculture, Environment and Rural Affairs in Northern Ireland.

Classification	MPC	Protein	Ash	Lactose	Moisture	Fat
LOW (≤50%)	**MPC40**	38.63 ± 0.40	6.20 ± 0.06	50.80 ± 0.07	4.07 ± 0.09	0.60 ± 0.00
MEDIUM (51≤%≤70)	**MPC50**	52.77 ± 0.25	6.73 ± 0.01	35.70 ± 0.09	4.14 ± 0.16	0.88 ± 0.00
	MPC60	62.85 ± 0.48	6.99 ± 0.01	25.00 ± 0.03	4.40 ± 0.21	1.06 ± 0.03
HIGH (≥71%)	**MPC70**	71.31 ± 0.52	7.21 ± 0.02	15.10 ± 0.09	5.66 ± 0.25	1.15 ± 0.13
	MPC80	80.94 ± 0.53	7.55 ± 0.01	5.28 ± 0.04	5.20 ± 0.20	1.46 ± 0.09

Table 1. MPC classification and composition (%, w/w) of MPC powders.

Pressure (Torr)	2.3	2.6	2.9	3.3	3.6	3.9	4.2	4.6	4.9	5.2	5.5	5.9	6.2	6.8

RH (%)	35	40	45	50	55	60	65	70	75	80	85	90	100	>100

Table 2. Relative humidity (RH, %) at 5°C constant from the appendix of Messier & Vitale (1993).

MPC	Initial swelling stage	Significant swelling stage	Particle fusion	Particle dissolution
40	50%	75-80%	90-95%	**YES**
50	50%	80-85%	90-95%	**YES** (a few undissolved particles' elements)
60	50%	85-90%	95-100%	**YES** (more undissolved particles' elements)
70	50%	85-90%	100%	**NO** (some particles undissolved)
80	50%	85-90%	>100%	**NO** (most particles undissolved)

Table 3. Relative Humidity (%) for the start of key stages of hydration to occur in MPC 40 to MPC80 at 5°C constant.

Figure 1. Saturated water vapour (100% RH) curve as a function of pressure (in Torr) and temperature (in °C). The physical state of water can be modified by changes in pressure and/or temperature. Points that lie above the curve represent the liquid phase, below the curve the gaseous phase.

Figure 2. ESEM micrographs showing surface microstructure of (a) MPC40, (b) MPC 50, (c) MPC60, (d) MPC70, (e) MPC80 at 5°C and 35%RH. Yellow arrows indicate dents/folds on the particle surface, light blue arrow MPC40 wrinkled surface, and the green arrow the particles' smooth surface. The black data bar displays prevailing operational parameters: ***det*** *is the detector used (GSED, gaseous secondary electron detector);* ***HV*** *is the accelerating voltage of the electron beam;* ***spot*** *is the beam spot size;* ***mag*** *for magnification;* ***WD*** *for working distance;* ***temp*** *is the temperature at sample level;* ***pressure*** *is the water vapour pressure (in torr) in the ESEM chamber; scale bar is presented.*

Figure 3. ESEM micrographs showing MPC40 hydration at 5°C. The white arrows indicate holes in MPC particles. (a) 35% RH (2.3 Torr), (b) 50%RH (4.6 Torr), (c) 80% RH (5.2 Torr), (d) 90% RH (5.9 Torr), (e) 100% RH (6.5 Torr), note the holes closing during this phase, (f) >100% RH (6.8 Torr).

Figure 4. ESEM micrographs showing MPC50 rehydration at 5°C. (a) 35% RH (2.3 Torr), (b) 50%RH (4.6 Torr), (c) 80% RH (5.2 Torr), (d) 90% RH (5.9 Torr), (e) 100% RH (6.5 Torr), (f) >100% RH (6.8 Torr).

Figure 5. ESEM micrographs showing MPC60 rehydration at 5°C. (a) 35% RH (2.3 Torr), (b) 50%RH (4.6 Torr), (c) 80% RH (5.2 Torr), (d) 90% RH (5.9 Torr), (e) 100% RH (6.5 Torr), (f) >100% RH (6.8 Torr).

Figure 6. ESEM micrographs showing MPC70 rehydration at 5°C. (a) 35% RH (2.3 Torr), (b) 50%RH (4.6 Torr), (c) 80% RH (5.2 Torr), (d) 90% RH (5.9 Torr), (e) 100% RH (6.5 Torr), (f) >100% RH (6.8 Torr).

Figure 7.ESEM micrographs showing MPC80 rehydration at 5°C. (a) 35% RH (2.3 Torr), (b) 50%RH (4.6 Torr), (c) 80% RH (5.2 Torr), (d) 90% RH (5.9 Torr), (e) 100% RH (6.5 Torr), (f) >100% RH (6.8 Torr).

Figure 8. ESEM micrographs showing MPC40 to MPC80, pre and post hydration at 5°C and 35% RH. Pre-hydration (a) MPC40, (b) MPC 50, (c) MPC60 (d) MPC70, (e) MPC80. Post-hydration, (f) MPC40, (g) MPC 50, (h) MPC60 (i) MPC70, (j) MPC80.

Figure 9. ESEM micrographs showing MPC80 (a) pre-hydration and (b) post-hydration at 5°C and 35% RH. Encircled areas represent the same region of interest in both images.

Supplementary materials:

Figure S1. Copper stub with the sample (MPC60) on top inside the microscope chamber (a) before and (b) after the RH increase (at over 100% RH). The arrow shows the "water droplet" that forms on top of the sample.

Figure S2. MPC80 particles floating on top of the "water droplet" at over 100% RH (a). With the droplet increase, the particles continue to float on top of it without sinking (b).

Videos:

Video 1. ESEM video showing surface microstructure of MPC40 at 5°C with RH increasing by 5% every 5 minutes interval (from 35% to over 100%). RH is shown at the top of each micrograph.

Video 2. ESEM video showing surface microstructure of MPC50 at 5°C with RH increasing by 5% every 5 minutes interval (from 35% to over 100%). RH is shown at the top of each micrograph.

Video 3. ESEM video showing surface microstructure of MPC60 at 5°C with RH increasing by 5% every 5 minutes interval (from 35% to over 100%). RH is shown at the top of each micrograph.

Video 4. ESEM video showing surface microstructure of MPC70 at 5°C with RH increasing by 5% every 5 minutes interval (from 35% to over 100%). RH is shown at the top of each micrograph.

Video 5. ESEM video showing surface microstructure of MPC80 at 5°C with RH increasing by 5% every 5 minutes interval (from 35% to over 100%). RH is shown at the top of each micrograph.

References:

1. Aguilar, & Ziegler (1994). Physical and microscopic characterization of dry whole milk with altered lactose content. 2. Effect of lactose crystallization. *Journal of Dairy Science*, 77(5), pp. 1198-1204. https://doi.org/10.3168/jds.S0022-0302(94)77058-2
2. Aguilera J., Valle J., & Karel M. (1995). Caking phenomena in amorphous food powders. *Trends in Food Sciences & Technology*, 6, pp. 149-155. https://doi.org/10.1016/S0924-2244(00)89023-8
3. Aguilera J.M. (1999). Simultaneous heat and mass transfer: dehydration. In Aguiilera J.M. & Stanley D.W. (Eds.), Microstructural Principles of Food Processing and Engineering, 2nd edition, Springer-Verlag US, pp. 373-411.
4. Anema S.G., Pinder D.N., Hunter R.J., & Hemar Y. (2006). Effects of storage temperature on the solubility of milk protein concentrate (MPC85). *Food Hydrocolloids*, 20, pp. 386-393. https://doi.org/10.1016/j.foodhyd.2005.03.015
5. Antonijevic M., Novac O., & O'Hagan B.M.G. (2018). Can emollients of similar composition be assumed to be therapeutically equivalent: a comparison of skin occlusivity and emulsion microstructure. *Clinical, Cosmetic and Investigational Dermatology*, 11, pp. 461-465. https://doi.org/10.2147/CCID.S176943
6. Auty M.A.E. (2018). Microscopy techniques for dairy products – An introduction. In El Bakry M., Sanchez A. & Mehta B.M. (Eds.). *Microstructure of Dairy Products.* John Wiley and Sons Ltd., pp. 1-32. https://doi.org/10.1002/9781118964194.ch1
7. Baldwin A.J., & Truong G.N.T. (2007). Development of insolubility in dehydration of dairy milk powders. *Food and Bioproducts Processing*, 85, pp. 202-208. https://doi.org/10.1205/fbp07008
8. Baldwin A.J. (2010). Insolubility of milk powder products – A mini review. *Dairy Science and Technology*, 90, pp. 169-179. https://doi.org/10.1051/dst/2009056

9. Berlin E., Anderson B.A., & Pallansch M.J. (1968). Comparison of water vapour sorption by milk powder components. *Journal of Dairy Science*, 51(12), pp. 1912-1915. https://doi.org/10.3168/jds.S0022-0302(68)87311-4
10. Bhandari B. (2013). Introduction of food powders. In Bhandari B., Bansal N., Zhang M., & Schuck P. (Eds.), Handbook of Food Powders: Processes and Properties. Woodhead Publishing Limited, Cambridge, UK, pp. 1-25. https://doi.org/10.1533/9780857098672.1
11. Bouvier J-M, Collado M., Gardiner D., Scott M., & Schuck P. (2013). Physical and rehydration properties of milk protein concentrates: comparison of spray-dried and extrusion-porosified powders. *Dairy Science and Technology*, 93, pp. 387-399. https://dx.doi.org/10.1007/s13594-012-0100-7
12. Buckman J.O. (2000). ESEM application note: wettability studies of Petroleum Reservoir Rocks. *Method.* https://dx.doi.org/10.13140/RG.2.1.1813.2246
13. Buma T.J. & Henstra S. (1971). Particle structure of spray-dried milk products as observed by a scanning electron microscope. *Netherlands Milk Dairy Journal*, 25, pp. 75-80.
14. Burgain J., Scher J., Petit J., Francius G., & Gaiani C. (2016). Links between particle surface hardening and rehydration impairment during micellar casein powder storage. *Food Hydrocolloids*, 61, pp. 277-285. https://doi.org/10.1016/j.foodhyd.2016.05.021
15. Burgain J., Petit J., Scher J., Rasch R., Bhandari B., & Gaiani C. (2017). Surface chemistry and microscopy of food powders. *Progress in Surface Science*, 92, pp. 409-429. https://doi.org/10.1016/j.progsurf.2017.07.002
16. Carić M., & Keláb M. (1987). Effects of drying techniques on milk powders quality and microstructure: a review. *Food Structure*, 6, pp. 171-180.

17. Carpin M., Bertelsen H., Bech J.K., Jeantet R., Risbo J., & Schuck P. (2016). Caking of lactose: a critical review. *Trends in Food Science & Technology*, 53, pp. 1-12. https://doi.org/10.1016/j.tifs.2016.04.002

18. Carpin M., Bertelsen H., Dalberg A., Bech J.K., Risbo J., Schuck P., & Jeantet R. (2017). How does particle size influence caking in lactose powder? *Journal of Food Engineering*, 209, pp. 61-67. http://dx.doi.org/10.1016/j.jfoodeng.2017.04.006

19. Crowley S.V., Gazi I., Kelly A.L., Huppertz T., & O'Mahony J.A. (2014). Influence of protein concentration on the physical characteristics and flow properties of milk protein concentrate powders. *Journal of Food Engineering*, 135, pp. 31-38. https://doi.org/10.1016/j.jfoodeng.2014.03.005

20. Crowley S.V., Desautel B., Gazi I., Kelly A.L., Huppertz T., & O'Mahony J.A. (2015). Rehydration characteristics of milk protein concentrate powders. *Journal of Food Engineering*, 149, pp. 105-113. https://doi.org/10.1016/j.jfoodeng.2014.09.033

21. Crowley S.V., Kelly A.L., Schuck P., Jeantet R., & O'Mahony J. A. (2016). Rehydration and solubility characteristics of high-protein dairy powders. In P. L. H. McSweeney, & J. A. O'Mahony (Eds.), Advanced Dairy Chemistry, Vol. 1: Proteins, part B, New York: Springer pp. 99-131. https://doi.org/10.1007/978-1-4939-2800-2

22. Danilatos G.D. (1985). Design and construction of an atmospheric or environmental SEM (part 3). *Scanning*, 7, pp. 26-42. https://doi.org/10.1002/sca.4950070102

23. Danilatos G.D. (1991). Review and outline of environmental SEM at present. *Journal of Microscopy*, 162(3), pp. 391-402. https://doi.org/10.1111/j.1365-2818.1991.tb03149.x

24. Davenel A., Schuck P., & Marchal P. (1997). A NMR relaxomentry method for determining the reconstitutability and the water-holding capacity of protein-rich milk powders. *Milchwissenschaft*, 52, pp. 35-39.

25. Donald A.M. (2003). The use of environmental scanning electron microscopy for imaging wet and insulating materials. Nature Mater, 2, pp. 511-516. https://doi:10.1038/nmat898

26. Fäldt P., & Bergenståhl B. (1994). The surface composition of spray-dried protein—lactose powders. *Colloids and Surfaces A: Physicochemical and Engineering Aspects*, 90, pp. 183–190. https://doi:10.1016/0927-7757(94)02914-8

27. Fang Y., Selomulya C., & Chen X.D. (2010). Characterization of milk protein concentrate solubility using focused beam reflectance measurement. *Dairy Science and Technology*, 90, pp 253-270. https://doi.org/10.1051/dst/2009050

28. Fang Y., Selomulya C., Ainsworth S., Palmer M., & Chen X.D. (2011). On quantifying the dissolution behaviour of milk protein concentrate. *Food hydrocolloids*, 25, pp. 503-510. https://doi.org/10.1016/j.foodhyd.2010.07.030

29. Felix da Silva D., Ahrné L., Ipsen R., & Hougaard A.B. (2018). Casein-based powders: characteristics and rehydration properties. *Comprehensive reviews in Food Science and Food Safety*, 17, pp. 240-254. https://doi.org/10.1111/1541-4337.12319

30. Fitzpatrick J.J., Barry K., Cerqueira P.S.M., Iqbal T., O'Neill J., & Roos Y.H. (2007). Effect of composition and storage conditions on the flowability on dairy powders. *International Dairy Journal*, 17, 383-392. https://doi.org/10.1016/j.idairyj.2006.04.010

31. Forny L., Marabi A., & Palzer S. (2011). Wetting, disintegration and dissolution of agglomerated water soluble powders. *Powder Technology*, 206, pp. 72-78. https://doi.org/10.1016/j.powtec.2010.07.022

32. Foster K.D., Bronlund J.E., & Paterson A.H.J. (2005). The contribution of milk fat towards the caking of dairy powders. *International Dairy Journal*, 15, pp. 85-91. https://doi.org/10.1016/j.idairyj.2004.05.005

33. Fyfe K.N., Kravchuk O., Le T., Deeth H.C., Nguyen A.V., & Bhandari B. (2011a). Storage induced changes to high protein powders: influence on surface properties and

solubility. *Journal of the Sciences of Food and Agriculture*, 91, pp. 2566-2575. https://doi.org/10.1002/jsfa.4461

34. Fyfe K., Kravchuk O., Nguyen A. V., Deeth H., & Bhandari B. (2011b). Influence of dryer type on surface characteristics of milk powders. *Drying Technology: An International Journal*, 29, pp. 758-769. https://doi.org/10.1080/07373937.2010.538481

35. Gaiani C., Banon S., Scher J., Schuck P., & Hardy J. (2005). Use of a turbidity sensor to characterize micellar casein powder rehydration: influence of some technological effects. *Journal of Dairy Sciences*, 88, pp.2700-2706.

36. Gaiani C., Scher J., Schuck P., Hardy J., Desobry S., & Banon S. (2006a). The dissolution behaviour of native phosphocaseinate as a function of concentration and temperature using a rheological approach. *International Dairy Journal*, 16, pp.1427-1434. https://doi.org/10.3168/jds.S0022-0302(05)72948-9

37. Gaiani C., Ehrhardt J.J., Scher J., Hardy J., Desobry S., & Bann S. (2006b). Surface composition of dairy powders observed by X-ray photoelectron spectroscopy and effects on their rehydration properties. *Colloids and surfaces*, 49, pp. 71-78. https://doi.org/10.1016/j.colsurfb.2006.02.015

38. Gaiani C., Schuck P., Desobry S., & Banon S. (2007). Dairy powder rehydration: influence of protein state, incorporation mode, and agglomeration. *Journal of airy Science*, 90, pp. 570-581. https://doi.org/10.3168/jds.S0022-0302(07)71540-0

39. Gaiani C., Morand M., Sanchez C., Tehrany E.A., Jacquot M., Schuck P., Jeantet R, & Scher J. (2010). How surface composition of high milk protein powders is influenced by spry-drying temperature. *Colloids and Surfaces B: Biointerfaces*, 75, pp. 377-384. https://doi.org/10.1016/j.colsurfb.2009.09.016

40. Garcia-Salinas M.J., & Donald A.M. (2010). Use of Environmental Scanning Electron Microscopy to image poly(N-isopropylcrylamide) microgel particles. *Journal of Colloid and Interface Science*, 342, pp. 629-635. https://doi.org/10.1016/j.jcis.2009.10.064

41. Gazi I., & Huppertz T. (2015). Influence of protein content and storage conditions on the solubility of caseins and whey proteins in milk protein concentrates. *International Dairy Journal*, 46, pp. 22-30. https://doi.org/10.1016/j.idairyj.2014.09.009

42. Haque M.K., & Roos Y.H. (2004). Water sorption and plasticization behavior of spray-dried lactose/protein mixtures. *Journal of Food Science*, 69, pp. E384-E391. https://doi.org/10.1111/j.1365-2621.2004.tb09900.x

43. Haque E., Bhandari B.R., Gidley M.J., Deeth H.C., Møller S.M., & Whittaker A.K. (2010). Protein conformational modifications and kinetics of water-protein interactions in milk protein concentrate powder upon aging: effect on solubility. *Journal of Agricultural and Food Chemistry*, 58, pp. 7748-7755. https://doi.org/10.1021/jf1007055

44. Haque E., Bhandari B.R., Gidley M.J., Deeth H.C., & Whittaker A.K. (2011). Ageing-induced solubility loss in milk protein concentrate powder: effect of protein conformational modifications and interactions with water. *Journal of the Sciences of Food and Agriculture*, 91, pp. 2576-2581. https://doi.org/10.1002/jsfa.4478

45. Hardy J., Scher J., & Banon S. (2002). Water activity and hydration of dairy powders. *Lait*, 72, pp. 441-452. https://doi.org/10.1051/lait:2002022

46. Havea P. (2006). Protein interactions in milk protein concentrate powders. *International Dairy Journal*, 16, pp. 415–422. https://doi.org/10.1016/j.idairyj.2005.06.005

47. Hogan S.A., & O'Callaghan D.J. (2010). Influence of milk proteins on the development of lactose-induced stickiness in dairy powders. *International Dairy Journal*, 20, pp. 121-221.

48. Huppertz T., Fox P.F. & Kelly A.L. (2018). 3 - The caseins: structure, stability, and functionality. Yada R. Y. (Ed.). In Woodhead Publishing Series in Food Sciences,

Technology and Nutrition, Proteins in Food Processing (second edition), pp. 49-92. https://doi.org/10.1016/B978-0-08-100722-8.00004-8

49. Ikeda S. (2015). Functional and hydration properties of milk protein concentrate (MPC). *Milk Science*, 64(2), pp 127-137. https://doi.org/10.11465/milk.64.127
50. James B. (2009). Advances in ‘‘wet’’ electron microscopy techniques and their application to the study of food structure. *Trends in Food Sciences and Technology*, 20, pp. 114-124. http://dx.doi.org/10.1016/j.tifs.2009.01.057
51. James B.J., & Smith B.G. (2009). Surface structure and composition of fresh and bloomed chocolate analysed using X-ray photoelectron spectroscopy, cryo-scanning electron microscopy and environmental scanning electron microscopy. *Food Science and Technology*, 42, pp. 929-937. https://doi.org/10.1016/j.lwt.2008.12.003
52. Jouppila K., Kansikas J., & Roos Y.H. (1997). Glass transition, water plasticization, and lactose crystallization in skim milk powder. *Journal of Dairy Science*, 80, pp. 3152-3160. https://doi.org/10.3168/jds.S0022-0302(97)76286-6
53. Jouppila K., & Roos Y.H. (1994). Glass transition and crystallization in milk powders. *Journal of Dairy Science*, 77, pp. 2907-2915. https://doi.org/10.3168/jds.S0022-0302(94)77231-3
54. Kelab M. (1979). Scanning electron microscopy of dairy products: an overview. *Scanning Electron Microscopy III*, pp. 261-272.
55. Keláb M. (1981). Electron microscopy of milk products: a review of techniques. *Scanning Electron Microscopy III*, pp. 453-472.
56. Keláb M. (1984). Artefacts in conventional scanning electron microscopy of some milk products. *Food microstructure*, 3, pp. 95-111.

57. Keláb M., Allan-Wojtas P., & Miller S.S. (1995). Microscopy and other imaging techniques in food structure analysis. *Trends in Food Sciences and Technology*, 6, pp. 177-186. https://doi.org/10.1016/S0924-2244(00)89052-4

58. Kelly G.M., O'Mahony J.A., Kelly A.L., Huppertz T., Kennedy D., & O'Callaghan D.J. (2015). Influence of protein concentration on surface composition and physico-chemical properties of spray-dried milk protein concentrate powders. *International airy Journal*, 51, pp. 34-40. https://doi.org/10.1016/j.idairyj.2015.07.001

59. Kim E.H.J., Chen X.D., & Pearce D. (2002). Surface characterization of four industrial spray-dried dairy powders in relation to chemical composition, structure and wetting property. *Colloids and Surfaces B: Biointerfaces*, 26, pp. 197-212. https://doi: 10.1016/S0927-7765(01)00334-4

60. Kim E.H.J., Chen X.D., & Pearce D. (2005). Effect of surface composition on the flowability of industrial spary-dried dairy powders. *Colloids and Surfaces B: Biointerfaces*, 46, pp. 182-187. https://doi:10.1016/j.colsurfb.2005.11.005

61. Kitching S., & Donald A.M. (1998). Beam damage of polypropylene in the environmental scanning electron microscope: an FTIR study. *Journal of Microscopy*, 190, pp. 357-365. https://doi.org/10.1046/j.1365-2818.1998.00346.x

62. Kneifel W., Paquin P., Abert T., & Richard J.P. (1991). Water-holding capacity of proteins with special regards to milk proteins and methodogical aspects – A review. *Journal of Dairy Science*, pp. 2027-2041.

63. Kneifel W., & Seiler A. (1993). Water-holding properties of ilk protein products – A review. *Food Structure*, pp. 297-308.

64. Lagrange V., Whitsett D., & Burris C. (2015). Global market for dairy proteins. *Journal of Food Science*, 80, pp. 16-22. https://doi.org/10.1111/1750-3841.12801

65. Lai H.M. & Schmidt S.J. (1990). Lactose crystallization in skim milk powder observed by hydrodynamic equilibria, scanning electron microscopy and ^{2}H nuclear magnetic resonance. *Journal of Food Science*, 55(4), pp. 994-999. https://doi.org/10.1111/j.1365-2621.1990.tb01582.x

66. Lloyd R.J., Chen D. & Hargreaves J.B. (1996). Glass transition and caking of spray-dried lactose. *International Journal of Food Science and Technology*, 31, pp. 305-311. https://doi.org/10.1046/j.1365-2621.1996.00352.x

67. Maidannyk V., McSweeney D.J., Hogan S.A., Miao S., Montgomery S., Auty M.A.E., & McCarthy N.A. 920200. Water sorption and hydration in spray-dried milk protein powders: selected physicochemical properties. *Food Chemistry*, 304, pp. 1-9. https://doi.org/10.1016/j.foodchem.2019.125418

68. McKenna A.B. (2000). Effect of processing and storage on the reconstitution properties of whole milk and ultrafiltered skim milk powders. PhD thesis, Massey University, Palmerson North, New Zealand. http://hdl.handle.net/10179/4587

69. McSweeney D.J., Maidannyk V., Montgomery S., O'Mahony J.A., & McCarthy N.A. (2020). The influence of composition and manufacturing approach on the physical and rehydration properties of milk protein concentrate powders. *Foods*, 9, pp. 1-14.

70. Messier P., & Vitale T. (1993). Cracking in albumen photographs: an ESEM investigation. *Microscopy Research and Technique*, 25, pp. 374-383. https://doi.org/10.1002/jemt.1070250505

71. Mimouni A., Deeth H.C., Whittaker A.K., Gidley M.J., & Bhandari B.R. (2009). Rehydration process of milk protein concentrate powder monitored by static light scattering. *Food Hydrocolloids*, 23, pp. 1958-1965. https://doi.org/10.1016/j.foodhyd.2009.01.010

72. Mimouni A., Deeth H.C., Whittaker A.K., Gidley M.J., & Bhandari B.R. (2010a). Investigation of the microstructure of milk concentrate powders during rehydration: alterations during storage. *Journal of Dairy Science*, 93, pp. 463-472. https://doi.org/10.3168/jds.2009-2369

73. Mimouni A., Deeth H.C., Whittaker A.K., Gidley M.J., & Bhandari B.R. (2010b). Rehydration of high-protein-containing dairy powder: slow- and fast-dissolving components and storage effects. *Dairy Science & Technology*, 90, pp. 335-344. https://doi.org/10.1051/dst/2010002

74. Mistry V.V., & Hassan H.N. (1991). Delactosed, high milk protein powder. 1. Manufacture and composition. *Journal of Dairy Sciences*, 74, pp. 1163-1169.

75. Mistry V.V., Hassan H.N., & Robinson D.J. (1992). Effect of lactose and protein on the microstructure of dried milk. *Food Structure*, 2, pp. 73-82.

76. Mulvihill D.M., & Ennis M.P., (2003). Functional milk proteins: production and utilization. In: Fox P.F., McSweeney P.L.H. (Eds.). Advanced dairy chemistry, Vol. 1, Proteins, Part B. Kluwer, New York, pp. 1175-1228.

77. Murrieta-Pazos I., Gaiani C., Galet L., Cuq B., Desobry S. & Scher J. (2011). Comparative study of particle structure evolution during water sorption: Skim and whole milk powders. *Colloids and Surfaces B: Biointerfaces*, 87(1), pp. 1-10. https://doi.org/10.1016/j.colsurfb.2011.05.001

78. Murrieta-Pazos I., Gaiani C., Galet L., Calvet R., Cuq B., & Scher J. (2012). Food powders: surface and form characterization revisited. *Journal of Food Engineering*, 112, pp. 1-21. https://doi.org/10.1016/j.jfoodeng.2012.03.002

79. Murrieta-Pazos I., Galet L., Rolland C., Scher J., & Gaiani C. (2013). Interest of energy dispersive X-ray microanalysis to characterize the surface composition of milk powder

particles. *Colloids and Surfaces B: Biointerfaces*, 111, pp. 242-251. https://doi.org/10.1016/j.colsurfb.2013.05.025

80. Nijdam J.J., & Langrish T.A.G. (2006). The effect of surface composition on the functional properties of milk powders. *Journal of Food Engineering*. 77, pp. 919-925. https://doi:10.1016/j.jfoodeng.2005.08.020
81. Palzer S. (2005). Effect of glass transition on the desired and undesired agglomeration of amorphous food powders. *Chemical Engineering Science*, 60, 3959-3968. doi:10.1016/j.ces.2005.02.015
82. Peleg M. (1977). Flowability of food powders and methods for its evaluation: a review. *Journal of Food Process Engineering*, pp. 303-328. https://doi.org/10.1111/j.1745-4530.1977.tb00188.x
83. Perea-Flores M.J., Chanona-Perez J.J., Terres-Rojas E., Calderon-Dominguez G., Garibay-Febles V., Alamilla-Beltran L., & Gutierrez-Lopez G.F. (2010). Microstructure characterization of milk powders and their relationship with rehydration properties. In Woo M.W., Mujumdar A.S. & Daud W.R.W. (Eds.), Spray Drying Technology, Vol. 1, Singapore, ISBN - 978-981-08-6270-1, pp. 197-218.
84. Prime D., Leaper M.C., Leach V., Jones J.R., Richardson D.J., Rielly C.D., & Stapley A.G.F. (2010). Caking behaviour of spray-dried powders – using scanning probe microscopy to study nanoscale surface properties. *Chemical Engineering & Technology*, 34(7), pp. 1104-1108. https://doi.org/10.1002/ceat.201000537
85. Roos Y.R., & Karel M.A. (1992). Crystallization of amorphous lactose. *Journal of Food Science*, 57, pp. 775-777. doi:10.1111/j.1365-2621.1992.tb08095.x
86. Saito Z. (1985). Particle structure in spray-dried whole milk and in instant skim milk powder as related to lactose crystallization. *Food Structure*, 4(2), pp. 333.340.

87. Schuck P., Mejean S., Dolivet A., Gaiani C., Banon S., Scher J., & Jeantet R. (2007). Water transfer during rehydration of micellar casein powders. *Lait*, 87, pp. 425-432. https://doi.org/10.1051/lait:2007016

88. Schuck P. (2011). Dehydrated Dairy products. Milk powder: physical and functional properties of milk powders. In Fuquay (Ed.),Encyclopedia of Dairy Sciences. Amsterdam, pp. 117-124. https://doi.org/10.1016/B978-0-12-374407-4.00122-9

89. Shrestha A.K., Howes T., Adhikari B.P., Wood B.J., & Bhandari B.R. (2007). Effect of protein concentration on the surface composition, water sorption and glass transition temperature of spray-dried skim milk powders. *Food Chemistry*, 104, pp. 1436-1444. https://doi.org/10.1016/j.foodchem.2007.02.015

90. Sikand V., Tong P. S., Roy S., Rodriguez-Saona L. E., & Murray B. A. (2011). Solubility of commercial milk protein concentrates and milk protein isolates. *Journal of Dairy Science*, 94, pp. 6194–6202. https://doi.org/10.3168/jds.2011-4477

91. Stokes D.J. (2012). Environmental scanning electron microscopy for biology and polymer science. *Microscopy and Analysis*, pp. 67-71.

92. Stokes D.J. (2013). Environmental scanning electron microscopy (ESEM): principles and applications to food microstructures. In Morris V.J., & Groves K. (Eds.), Food microstructures, microscopy, measurement and modelling, pp. 3-26, ISBN 9780857095251, Woodhead Publishing.

93. Tai S.S.W., & Tang X.M. (2001). Manipulating biological samples for environmental scanning electron microscopy observation. *Scanning*, 23, pp. 267-272. doi:10.1002/sca.4950230407

94. Thomas M.E.C., Scher J., Desobry-Banon S., & Desobry S (2004). Milk powders ageing: effect on physical and functional properties. *Critical reviews in Food Science and Nutrition*, 44, pp. 297-322. doi:10.1080/10408690490464041

95. Timp, W., & Matsudaira, P. (2008). Electron Microscopy of Hydrated Samples. In Wilson L., & Matsudaira P. (Eds.), Biophysical tools for biologists, Vol. 2: In vivo techniques, pp. 391-407. https://doi.org/10.1016/S0091-679X(08)00614-6

96. Vignolles M.L., Jeantet R., Lopez C., & Shuck P. (2007). Free fat, surface fat and dairy powders: Interactions between process and product. A review. *Lait*, 87, pp. 187-236. https://doi.org/10.1051/lait:2007010

97. Vos B., Crowley S.V., O'Sullivan J., Evans-Hurson R., McSweeney S., Kruse J., M. Rizwan Ahmed, Fitzpatrick D., & O'Mahony J.A (2016). New insights into the mechanism of rehydration of milk protein concentrate powders determined by Broadband Acoustic Resonance Dissolution Spectroscopy (BARDS). *Food Hydrocolloids*, 61, pp 933-945. https://doi.org/10.1016/j.foodhyd.2016.04.031

98. Warburton S., & Pixton S.W. (1978). The moisture relations of spray dried skimmed milk. *Journal of Stored Products Research*, 14, pp. 143-158. https://doi.org/10.1016/0022-474X(78)90009-7

99. Zayas J.F. (1997). Water holding capacity of proteins. In Zayas J.F. (Ed.), Functionality of proteins in food, Springer-Verlag Berlin Heidelberg, pp. 73-133. https://doi.org/10.1007/978-3-642-59116-7_3

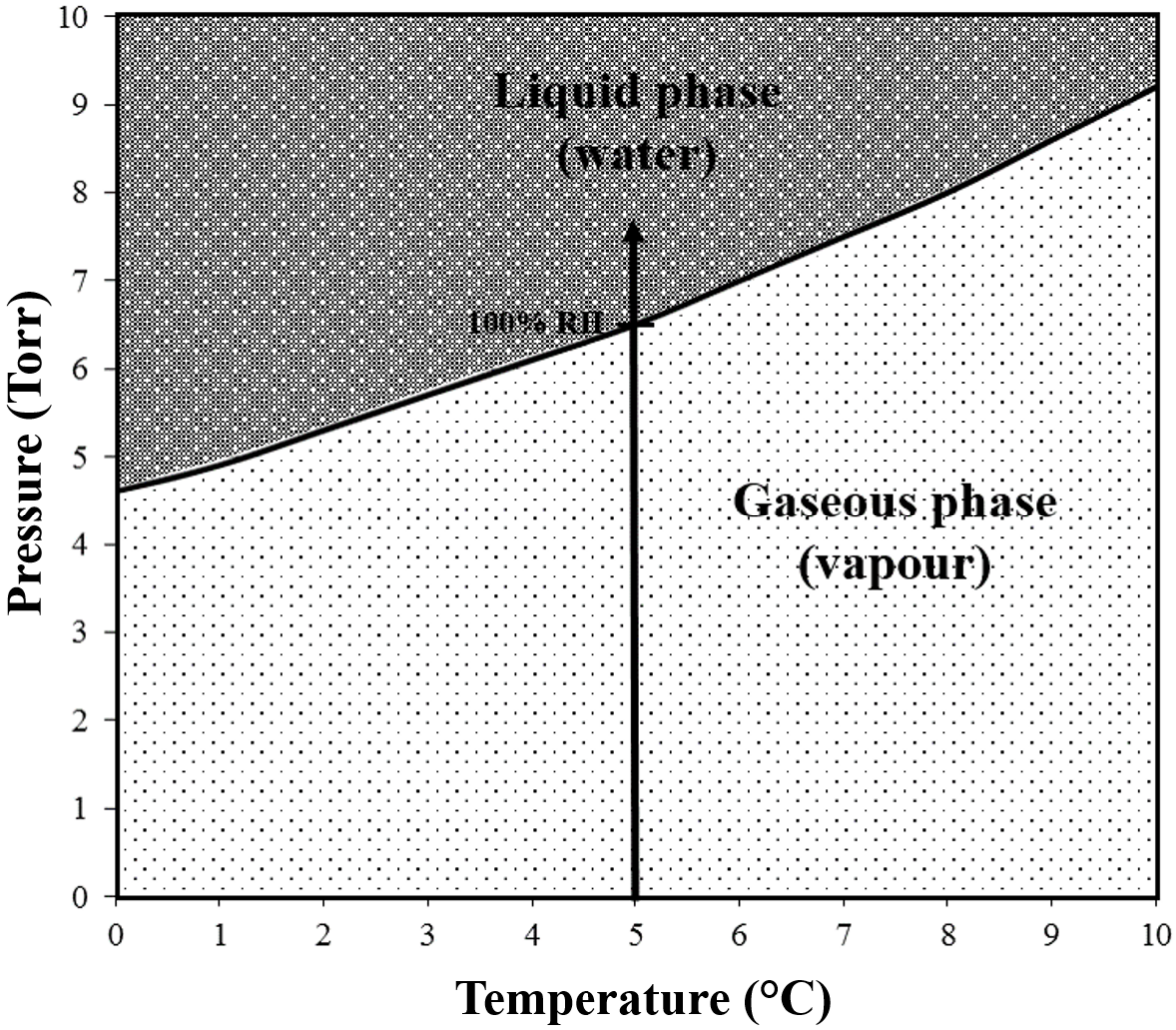
Liquid phase
(water)
100% RH
Gaseous phase
(vapour)
Pressure (Torr)
Temperature (°C)
0
1
2
3
4
5
6
7
8
9
10

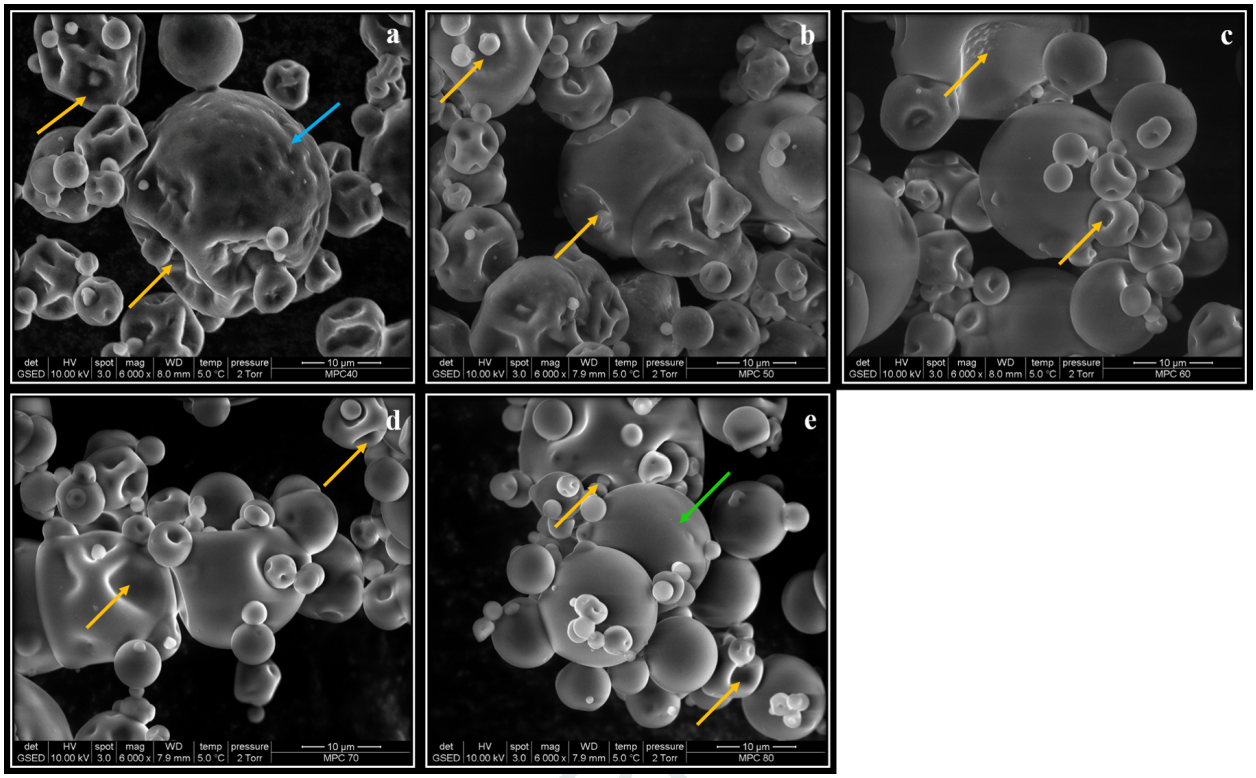

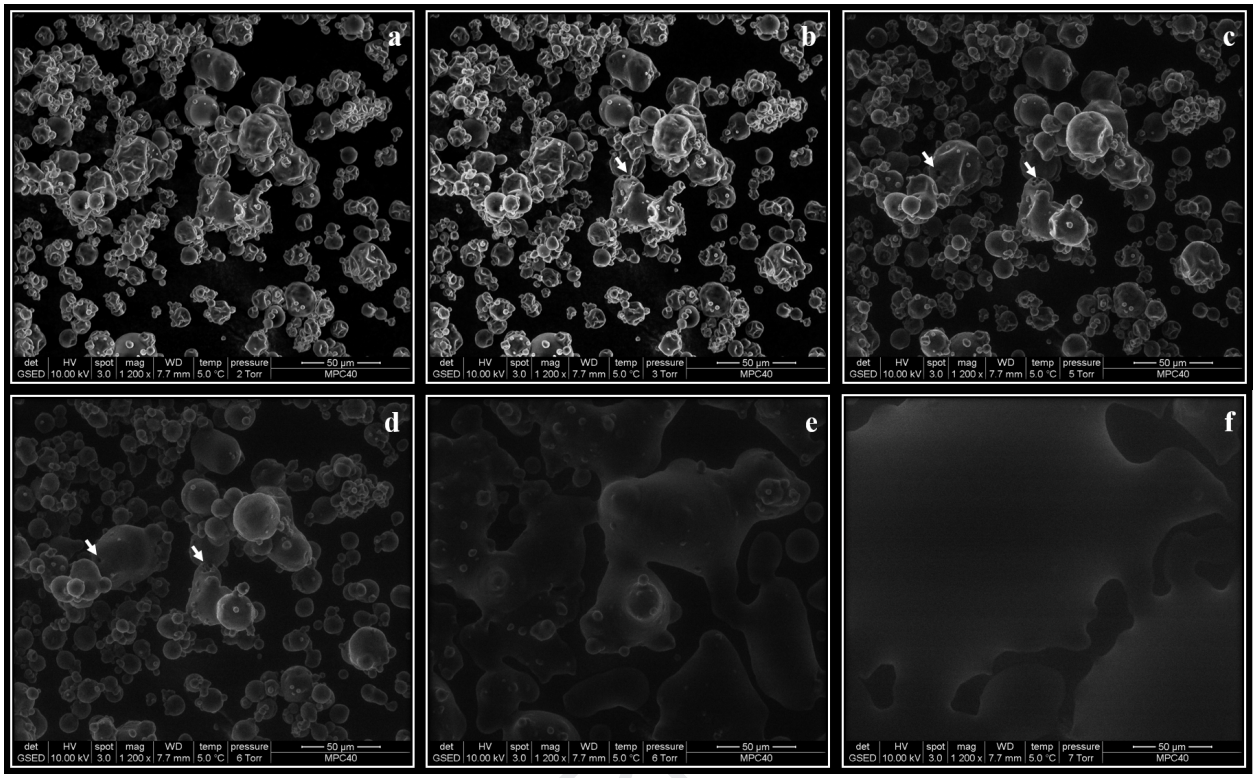

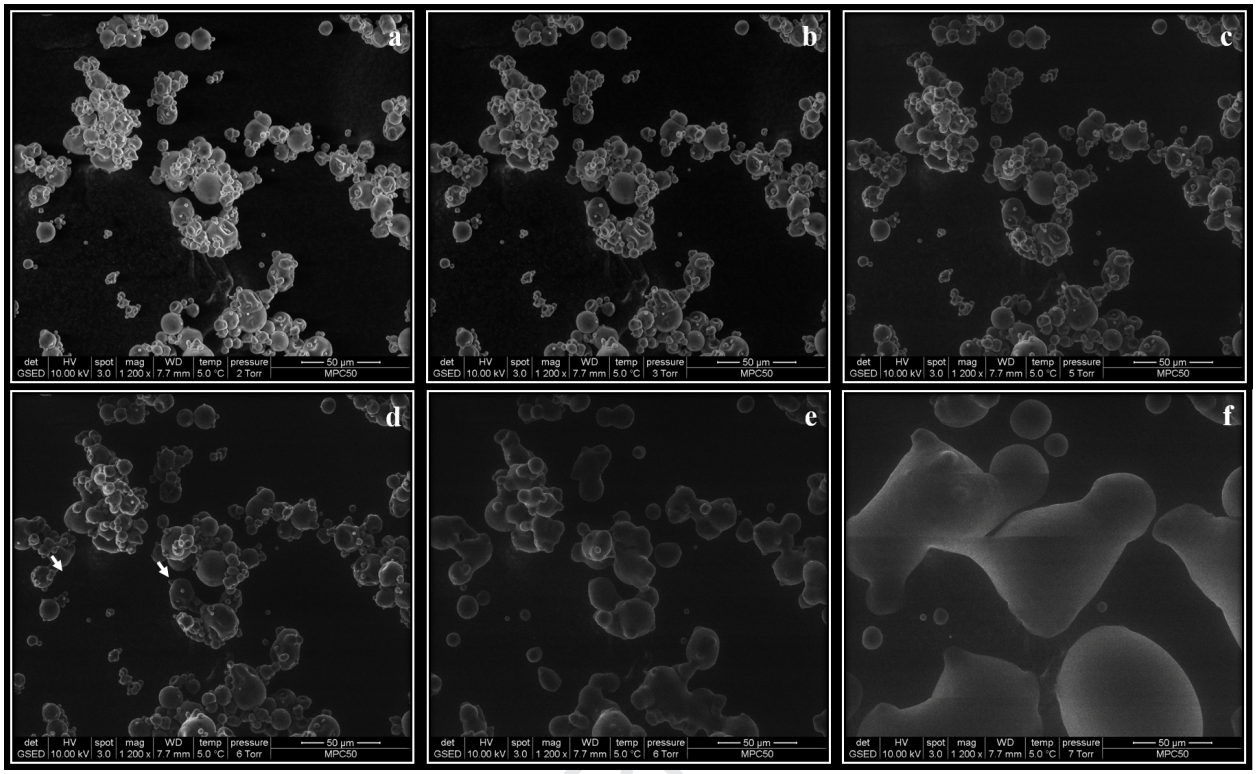

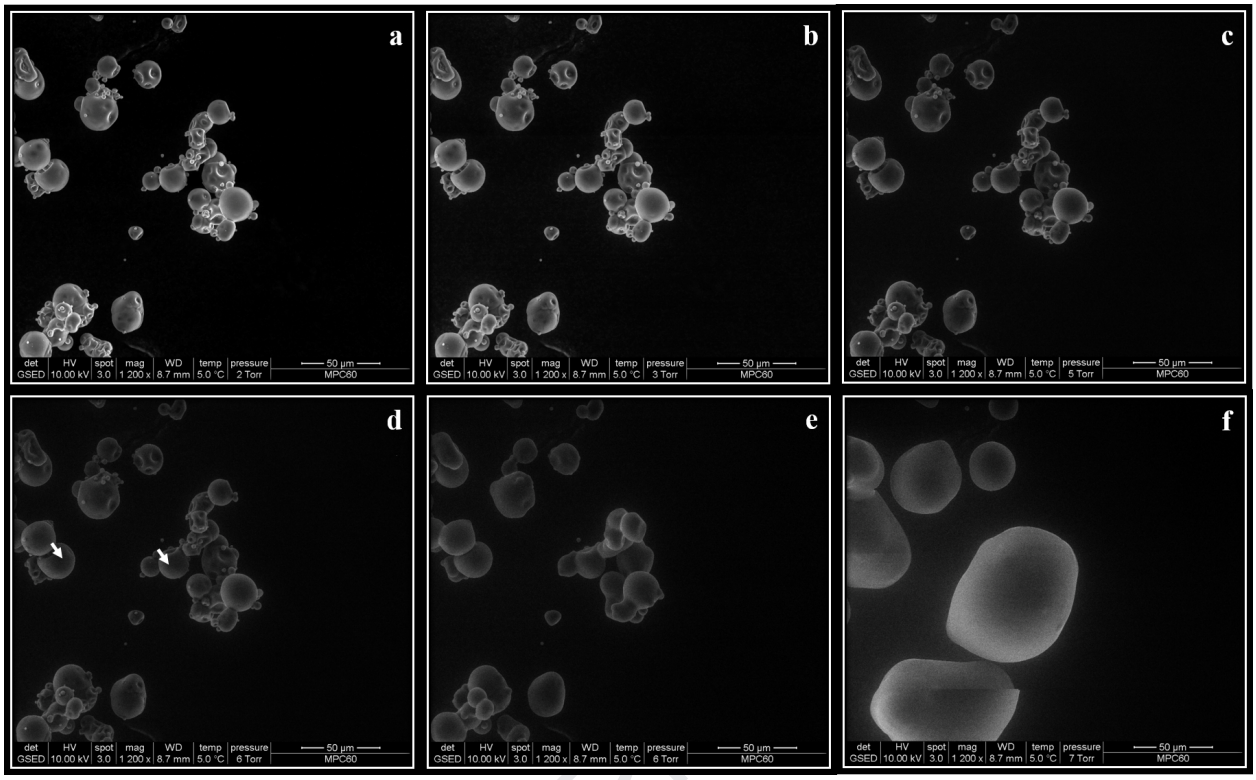

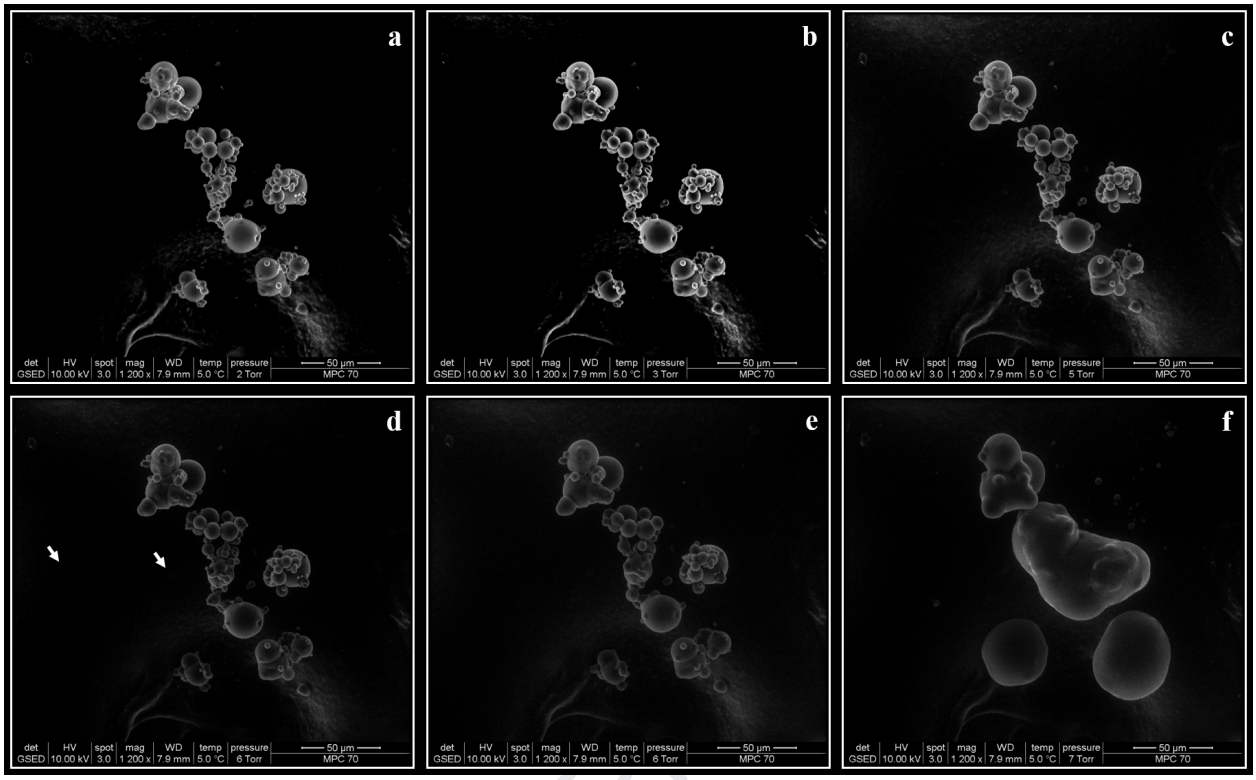

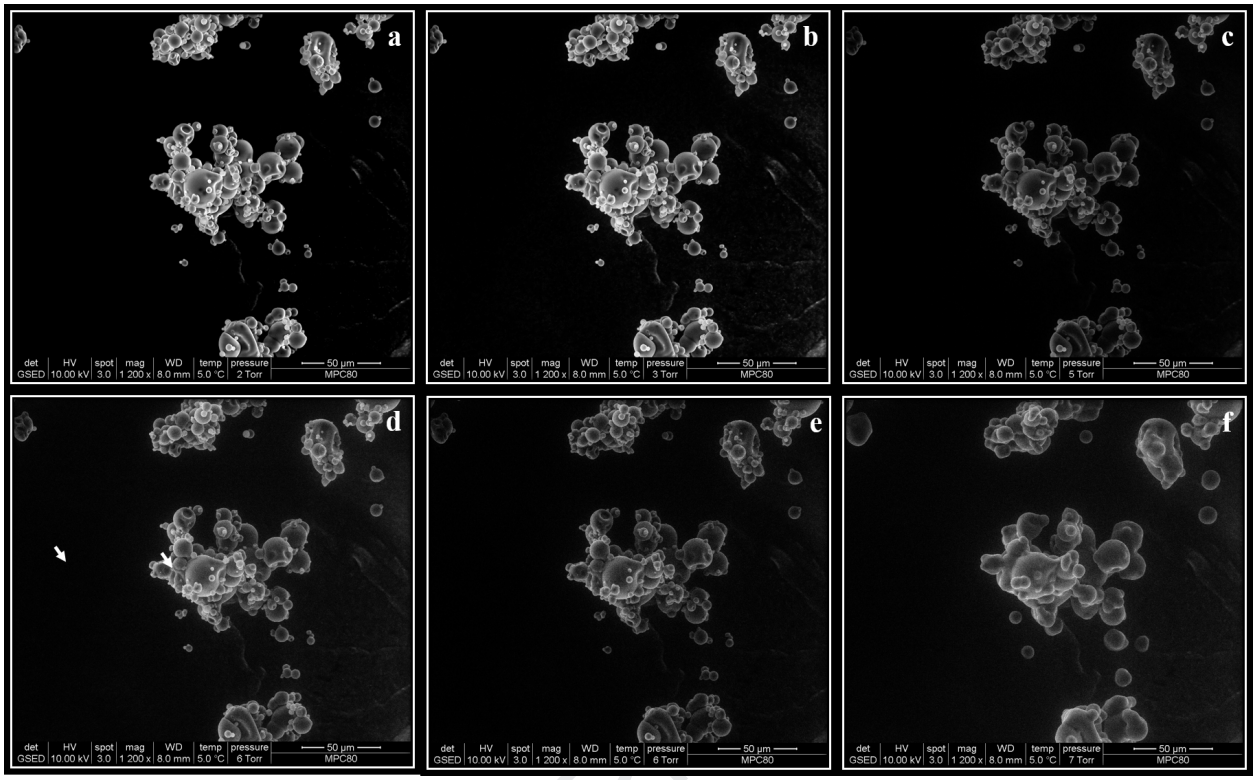

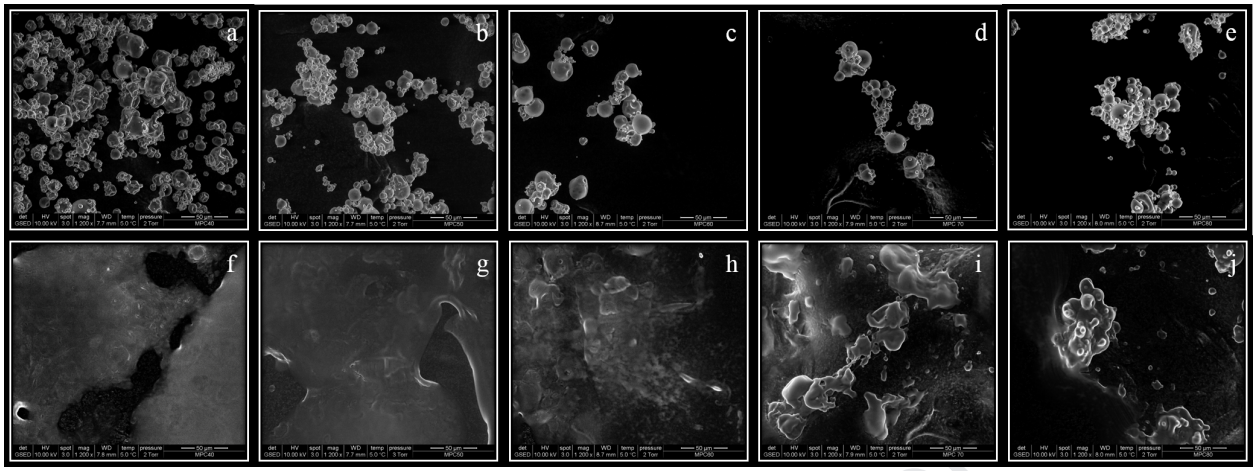

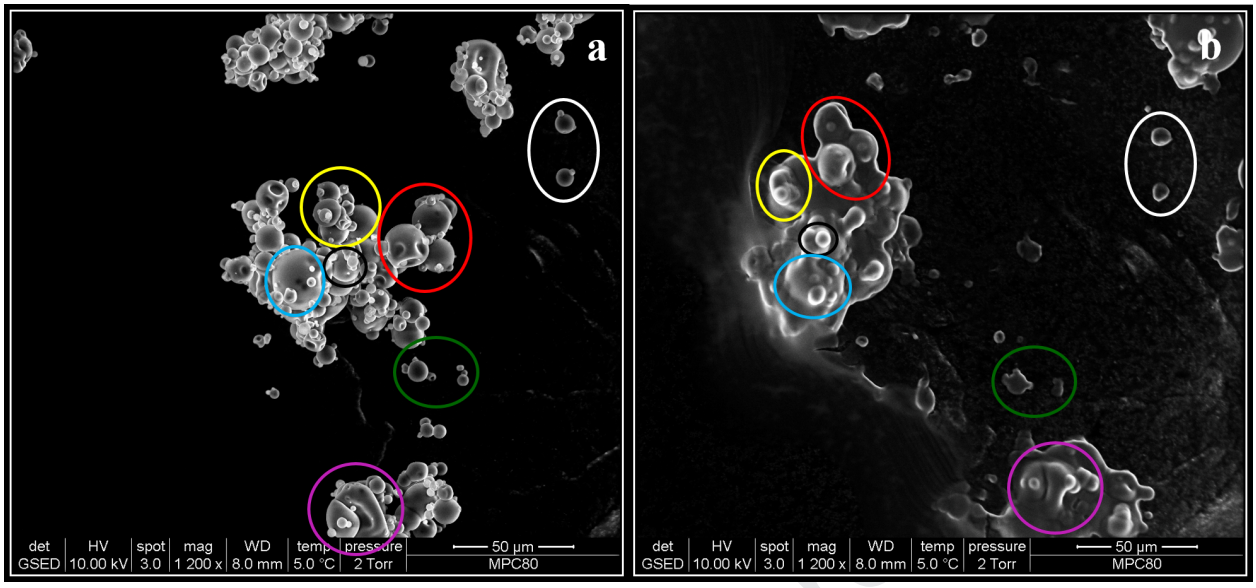

Highlights

- A novel method to image MPC surface during hydration and reconstitution by ESEM
- Real-time characterisation of the hydration process in at by ESEM
- Dynamic particle surface fusion and re-arrangement was observed during hydration
- At high relative humidity viscous bridges form between particles (fusion)
- Surface re-arrangement is the rate limiting step for MPC hydration

I confirm that this research has not been previously published or is currently submitted for publication elsewhere. All authors have approved the manuscript and agree with submission to *Food Hydrocolloids*. This original research was supported by the Food Institutional Research Measure (FIRM) project “Developing the next generation of high protein spray dried powders with enhanced hydration properties” (DAIRY DRY 15-F-679), funded by both the Irish Department of Agriculture, Food and the Marine and the Department of Agriculture, Environment and Rural Affairs in Northern Ireland. The funding resources had no involvement in the study design, data collection, analysis and interpretation, in the writing of the report or the decision to submit the article for publication. Declarations of interest: none.